Synthesis and electrochemical characterisation of Conducting polyaniline-fly ash matrix composites

By

Sipho Enos Mavundla

A thesis submitted in partial fulfilment of the requirement for the degree of

MAGISTER SCIENTIAE

UNIVERSITY of the
WESTERN CAPE

in the

Department of Chemistry

Faculty of Science

University of the Western Cape

November 2005

Supervisor: **Prof. E. Iwuoha**

DECLARATION

I declare that the Synthesis and electrochemical characterisation of Conducting polyaniline-fly ash matrix composites is my work, that has not been submitted for any degree or examination in any other university, and that all sources I have used or quoted have been indicated and acknowledged by complete references.

Sipho Enos Mavundla

Signature: ……

Date: ……

UNIVERSITY of the
WESTERN CAPE

Keywords: Electrochemical impedance spectroscopy, cyclic voltammetry, fly ash, polyaniline nanorods, polyaniline nanofibers, polystyrene sulphonic acid, polyaniline-fly ash composites, scanning electron microscopy, charge transfer coefficient, standard rate constant.

ABSTRACT

The aim of this study was to produce useful composite materials from fly ash, a major waste product of coal combustion from power plants. Polyaniline-fly ash (PANI-FA) composites were prepared by *in situ* polymerisation of aniline in the presence of Fly Ash (FA) by two slightly different methods. In one case polystyrene sulphonic acid (PSSA) was used as a stabilizer and in another case the starting materials (aniline and FA) were aged before oxidation. The aging procedure formed nanotubes that have cross-sectional diameters of 50-110 nm. The other procedure produced nanotubes with a diameter of 100-500 nm and the length of up to 10μm. The presence of metal oxides and silica in FA were responsible for the formation of nanorods in PANI-PSSA-FA.. The formation of the composites was confirmed by UV-Vis and FTIR. The UV-Vis showed maximum absorbance at 330-360 nm (due to π-π* transition of benzoid rings) and 600-650 nm(due to charge transfer excitons of quinoid rings), which are characteristics of emaraldine base. The electrochemical analysis of the composites showed that the composites were conductive and electroactive. The Cyclic Voltammetry of PANI-PSSA-FA showed three redox couples which are characteristics of sulphonated PANI. The morphology of the composites was studied by Scanning Electron Microscopy (SEM) and showed that our methods gave composites with improved homogeneity as compared to other reported methods. Thermo Gravimetric analysis (TGA) showed that the presence of FA in the composites improves the thermal stability of the composites by up to 100 ^{0}C.

UNIVERSITY of the
WESTERN CAPE

ACKNOWLEDGEMENTS

I would like to thank the following people for their contribution during my study:

My supervisor, Professor Emmanuel Iwuoha for his guidance, understanding, and for always lending a helping hand in times of trouble.

Dr Priscilla Baker and Dr Amir Al-Ahmed for their useful advices.

Ms Leslie Petrik, thank you very much for recommending me for a bursary.

I will also like to thank my colleagues in Sensor Research Laboratory and in Chemistry Department for their support.

I will not forget to thank my family and friends for their continuous support and encouragement.

I would like to thank Council for Scientific and Industrial Research (CSIR) and National Research Foundation (NRF) for their financial support.

Last but not the least: I would like to thank God for without him nothing is possible.

UNIVERSITY of the
WESTERN CAPE

TABLE OF CONTENTS

Declaration **i**

Abstract **ii**

Acknowledgements **iii**

Table of contents **iv**

1. Introduction 1

1.1. Conducting polymers 1

1.2. Polyaniline (PANI) 2

1.3. Doping 4

1.4. Applications of conducting polymers 6

1.5. Fly Ash 8

1.6. Composite Materials 12

1.6.1 Inorganic-Organic 13

1.6.2. Organic-Inorganic 13

Chapter 2 **16**

Literature Review **16**

2. Introduction 16

2.1. Polyaniline-Fly ash composites 16

2.2. Polyaniline nanocomposites 17

2.3. Polyaniline nanotubes 18

2.3.1. Synthesis 19

2.3.2. Formation mechanism 19

UNIVERSITY of the WESTERN CAPE

2.4. Electrochemical characterisation: background 22

2.4.1. Cyclic Voltammetry 22

2.4.2. Electrochemical Impedance 25

2.4.2.1. Circuit Elements 30

2.4.2.2. Equivalent Circuits 32

Chapter 3 **36**

Experimental **36**

3. Introduction 36

3.1. Synthesis procedure 36

3.1.1. Synthesis of PANI-FA composites 37

3.1.2. Synthesis of PANI-FA aged composites 37

3.1.3. Synthesis of PANI-PSSA-FA composites 38

3.1.4. Synthesis of PANI-PSSA-FA composites 38

3.2. Characterization 39

3.2.1. 3.2.1. Cyclic Voltammetry 39

3.2.2. Electrochemical Impedance 39

3.2.3. UV-Vis 40

3.2.4. FT-IR 40

3.2.5. Scanning Electron Microscopy 41

3.2.6. Thermal Gravimetric 41

Chapter 4 **42**

Results and discussion **42**

4. Introduction 42

UNIVERSITY of the
WESTERN CAPE

4.1. FT-IR 42

4.2. UV-Vis 45

4.3. Cyclic Voltammetry 51

4.4. Electrochemical Impedance 66

4.5. Scanning Electron Microscopy 71

4.6. Thermal Gravimetric Analysis 76

Chapter 5 **80**

5. Conclusion 80

Reference **83**

Appendix

List of Publications

Appendix 1.

UNIVERSITY of the
WESTERN CAPE

Electrochemical and Spectroscopic Properties of Fly Ash-Polyaniline Matrix Nanorod Composites.

Authors: Sipho E Mavundla, Emmanuel I. Iwuoha, Vernon S Somerset, Leslie F Petrik, Michael J. Klink, and Priscilla Bakers

Published in Microchimica **Acta.**

CHAPTER 1

INTRODUCTION

1.1. Conducting polymers

The discovery of conducting polymers dates back in the 1970s when a student of a Japanese professor Shirakawa, made a mistake by putting too much catalyst in the polymerisation of acetylene. This resulted in the formation of a silvery film instead of a black powder. When MacDiarmid heard about this, he invited Shirakawa to his laboratory at the University of Pennsylvania. They tried to modify the polyacetylene by oxidation with iodine vapour, which changed the optical properties of the material. They asked Heeger to have a look at the conductivity and he found that the conductivity has increased ten million times [1]. The discovery by these professors was considered a major break through in science; this earned them a noble prize in Chemistry in 2000. Since then the field has grown immensely, and also given rise to many new and exciting applications. The conducting polymers have conjugated double bonds in their backbone. There are many different types of conducting polymers. Figure 1 below shows the most common conducting polymers [2].

UNIVERSITY of the
WESTERN CAPE

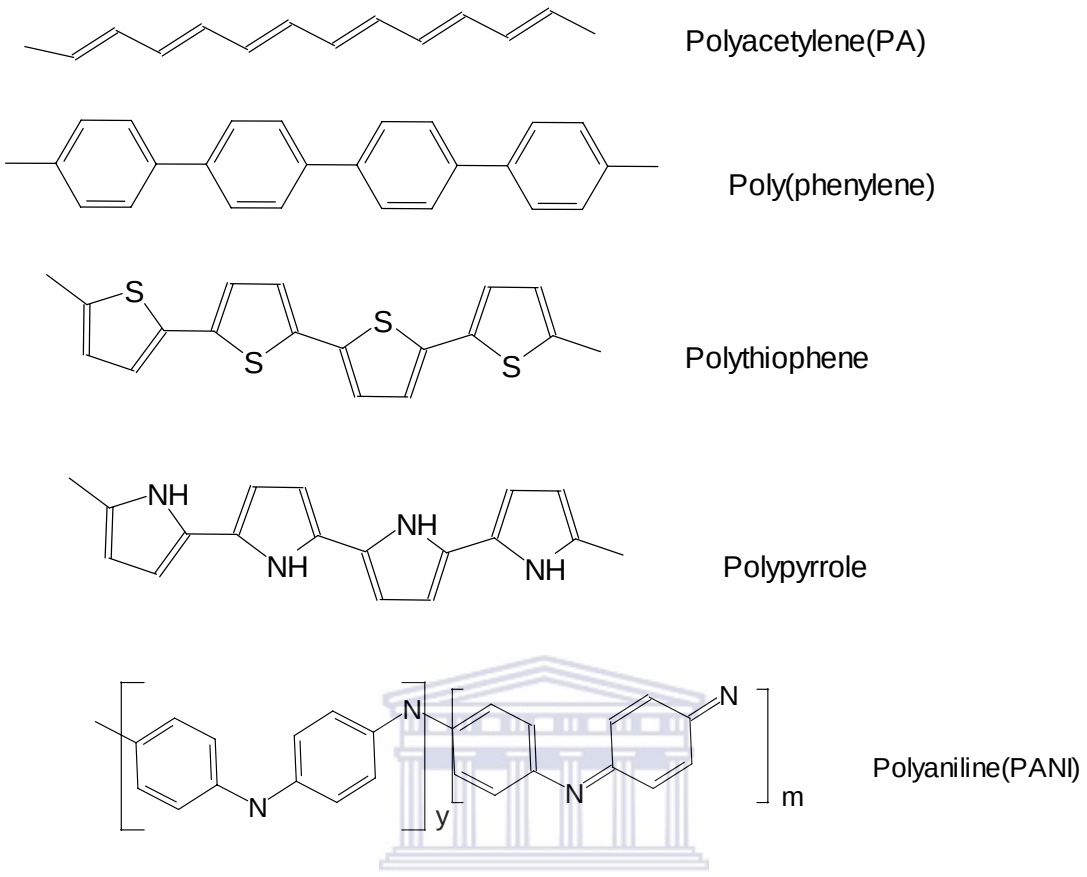

UNIVERSITY of the
WESTERN CAPE

Figure 1.1. Some examples of conducting polymers

1.2. Polyaniline (PANI)

Owing to its high conductivity, environmental stability and low cost of production, polyaniline (PANI) has been the subject of much investigation compared to other conducting polymers. PANI can be synthesized electrochemically or chemically by using an appropriate oxidant in an acidic medium. There are three forms of PANI, fully oxidized pernigraniline, half-oxidized emaraldine base (EB), and fully reduced leucoemaraldine base (LB) [1-3]. Emaraldine is said to be the most stable form of PANI and it is the most conductive form when it is doped (emaraldine salt).

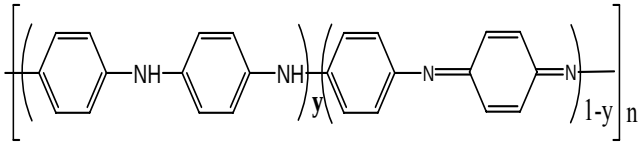

Figure 1.2. General structure of polyaniline. The completely reduced form (leucoemaraldine) can be obtained when (1-y) =0. The completely oxidized form (pernigraniline) when (1-y) =1 and when (1-y) =0.5 it corresponds to emaraldine base

PANI has many potential applications, in nanowires, electronics, electrochromic devices, batteries [3-10], etc., but all these applications are limited by the difficultly to process PANI. PANI itself is difficult to process; it does not dissolve in common solvent and it decomposes before melting. Many studies have been done in an effort to make PANI processable such as addition of side chain to the monomer aniline or doping with bulky dopants to make PANI soluble [5]. The problem with these bulky dopants was the solvent toxicity and difficult preparation [5].

UNIVERSITY of the
WESTERN CAPE

Another way to overcome the problem of processability is to prepare its nanocomposites or nanotubes/rods. Polyaniline has been used in many cases for synthesis of nanocomposites and nanotubes/rods by using clay, transitional metals oxides such as titanium oxide (TiO_2), vanadium oxide (V_2O_5), tin oxide [11-14] etc. These nanocomposites can be prepared chemically or electrochemically. The potential of polyaniline transitional metals nanocomposites have introduced these materials into applications such as electronic devices, non-linear optical systems and photo electrochemical systems [9]. It is believed that the combination of n-type semiconductor of transitional metals and p-type of PANI is responsible for the improvement in the

polyaniline photo current values due to the occurrence of excitons dissociation at the interface

1.3. Doping

For a polymer to be electrically conductive it must behave like a metal, that is, it must have free electrons that are mobile. The basic requirement is that the material must have conjugated double bonds, in addition , the electrons must be disturbed- by removing electrons (oxidation) or by inserting one (reduction). This process is called doping. Doping is reversible with little or no degradation of the polymer backbone. During this process the polymer, which is an insulator or semiconductor, is converted to metallic polymer, which is conductive. The conductivity can be increased up to 100 fold by this process of doping. Whether the polymer is doped chemically or electrochemically, the doping can be divided into two: *p*-doping (oxidation) and *n*-doping (reduction)

UNIVERSITY of the
WESTERN CAPE

p- type of doping is the partial oxidation of the polymer π backbone [5]. This was discovered by treating the polyacetylene with iodine (the oxidizing agent). In the *p*-type doping the electron is removed from the polymer backbone as described above. *n*-type doping is the partial reduction of the polymer π backbone. It was also discovered when polyacetylene was treated with reducing agent (liquid sodium). Like in the oxidation, the electron is inserted in the π backbone and the polymer becomes negatively charged. The negative ion will move along the polymer backbone with the help of solitons.

Doping is reversible with little or no degradation of the polymer backbone.

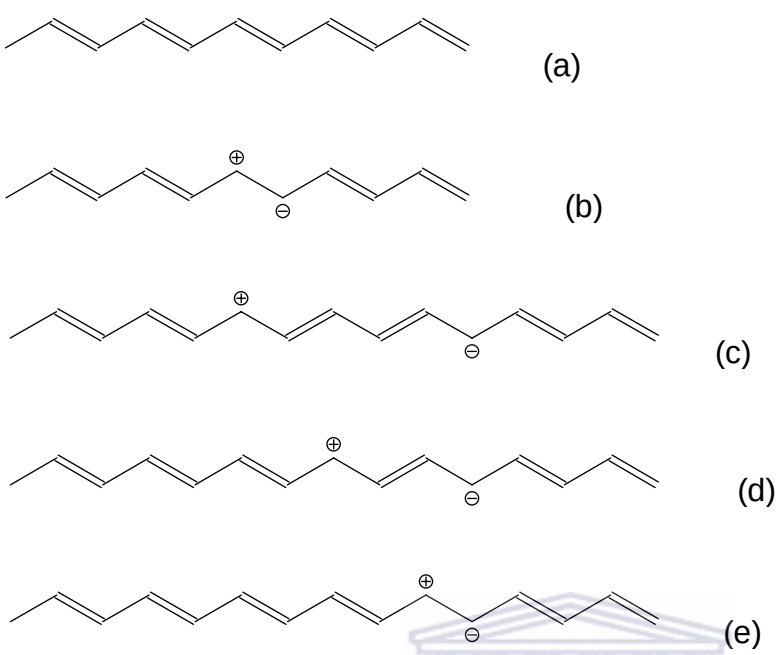

Figure. 1.3. Schematic representation of movement of charge along the polymer backbone.

UNIVERSITY of the
WESTERN CAPE

When the polymer is oxidized, the oxidizing agent attracts an electron from the polymer chain [1]. The polymer will now become positively charged; this is termed radical cation or polaron. The lone electron of the polymer double bond, from which an electron was removed, can move easily. As a consequence, the double bond successively moves along the molecule. When the polymer chain is strongly oxidized the polarons condense pair-wise into so-called solitons. These solitons are responsible for charge transport along the polymer backbone

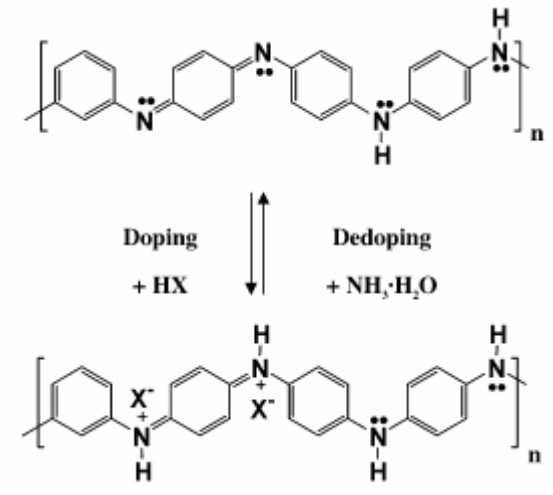

Figure 1.4. Doping and dedoping of PANI

1.4. Applications of conducting polymers

UNIVERSITY of the
WESTERN CAPE

The electrochemical and electronic behaviour of conducting polymers give rise to many possible applications to many devices including diodes, rechargeable battery electrodes, electrochromic display, anticorrosion protection, and sensors [8]. Many of the possible applications for conducting polymers rely on their electroactivity, i.e. reversible electrochemical doping. Polyaniline was the first conducting polymer to be commercially used in the rechargeable batteries in 1987[1]. Its potential came after it was realized that polyacetylene was not suitable for batteries because of its lack of stability in air, and brittleness.

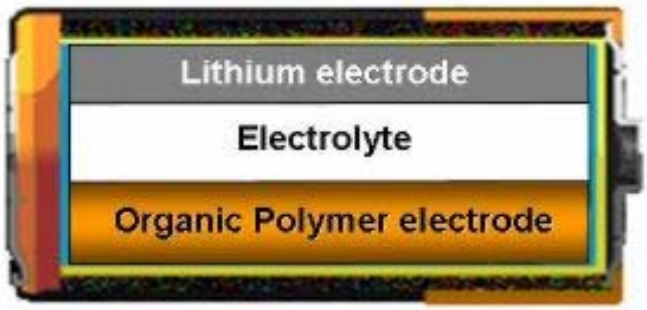

Figure 1.5. Example of conducting polymer rechargeable battery

Another promising application of PANI is in electrochromic devices. It is the ability of conducting polymers to change colour associated with redox reaction that has given conducting polymers the potential to be applied in electrochromic devices. The polyaniline changes from yellow- blue, blue –blue black, blue black-green upon the application of redox potential from -0.2 to 1 V [2]. In electrochromic devices a substance is customary adsorbed onto a transparent conducting substrate such as indium tin oxide glass, or kept in the solution between transparent electrodes.

UNIVERSITY of the
WESTERN CAPE

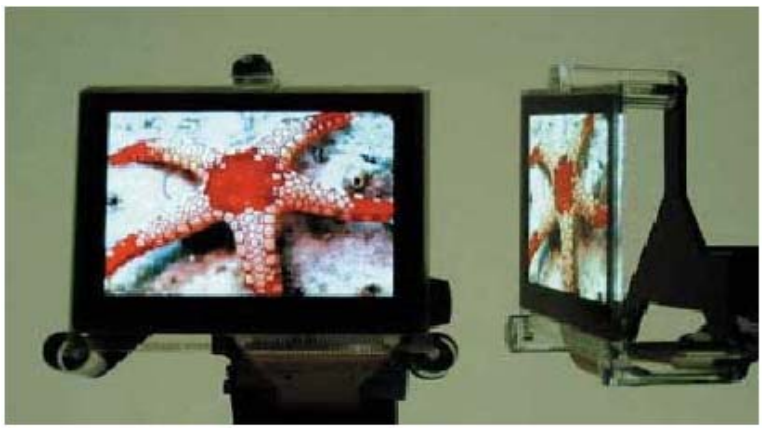

Figure 1.6. Example of electrochromic devices

The ability of PANI to change from being conducting to insulating by doping and dedoping process has earned its usage in anticorrosion protection. The stainless steel was the first metal to be used to test whether PANI can prevent corrosion [14]. Although PANI passed the test it was subsequently found that the undoped form of PANI performs better as anticorrosion agent. . Application of PANI in biosensor is very promising [15] where polyaniline is used both as an immobiliser and electron transfer mediator in amperometric sensors.

1.5. Fly Ash

Fly Ash (FA) is produced as a by-product when coal is burned for electric power generation. It is collected by control device systems, such as electrostatic precipitators and bag filters or allowed to escape into the atmosphere [6]. It is an alkaline grey powder with pH ranging from 9 to 9.9 [4,16,17]. There are a large number of coal-based power plants all over the world, creating a huge quantity of FA causing serious environmental problems. Less than half of the ash is used as a raw material for concrete manufacturing and construction and the remaining is directly dumped to land fill or simply pilled up. Particularly in South Africa about 90 % of electricity is produced by burning of coal, which disposes a huge amount of FA (~ 17 million m^3per annum)[16]. So to save our environment, new ways to utilizing the FA need to be explored.

UNIVERSITY of the
WESTERN CAPE

Figure 1.7. Coal fired power station.

UNIVERSITY of the
WESTERN CAPE

The main matrix elements in fly ash are Si, Al and Fe, together with significant percentages of Ca, Na, Mg and Ti. Fly Ash also contains some trace elements (Ba, Cu, Sr, Ni, Cr, Zn, Cd, Mo, V, Hg, Se, Pb, As), which are toxic [16]. Table 1 below shows the XRF results of different kinds of South African fly samples.

TABLE 1. XRF results of different kinds of South African FA

Elements	Matla	Lethabo	Kendal	Plasfil 5	Plasfil 15	Tailings 45/110	Plasfil 5/45
SiO_2	49.117	51.912	48.506	48.489	51.322	52.264	52.615
TiO_2	2.283	2.160	2.243	2.375	2.258	2.099	2.201
Al_2O_3	29.870	31.288	32.341	33.871	32.369	29.488	30.994
Fe_2O_3	4.318	5.399	5.733	4.772	4.747	5.835	5.078
Cr_2O_3	0.064	0.066	0.059	0.086	0.119	0.061	0.060
MnO	0.059	0.080	0.070	0.086	0.078	0.083	0.074
MgO	2.444	1.375	1.981	1.502	1.347	1.273	1.330
NiO	0.013	0.017	0.019	0.025	0.034	0.017	0.022
CaO	6.609	4.588	4.709	4.528	4.260	4.713	4.732
Na2O	0.667	0.372	0.450	0.398	0.439	0.413	0.448
K2O	0.957	0.538	0.698	0.636	0.577	0.540	0.634
P_2O_5	1.017	0.340	0.728	0.639	0.388	0.236	0.324
SO_3	0.672	0.179	0.553	0.218	0.217	0.123	0.185
H_2O-	0.047	0.044	0.160	0.074	0.032	0.020	0.023
LOI	1.046	1.590	1.303	1.734	1.360	1.927	0.997
Sum	99.183	99.948	99.551	99.433	99.547	99.092	99.716

UNIVERSITY of the
WESTERN CAPE

Fly Ash is disposed in two ways: dry disposal, where fly ash is removed in dry form to the place of disposal (Figure 2.19) [16, 18]. This causes air pollution and soil pollution. Another way is to dispose it is in a slurry form. This is more dangerous as this causes pollution of the undergroundwater due to metal leaching. In 2001 Eskom (the major power plant in South Africa) produced 27 megatons of fly ash [16]. From the millions of tones of South African FA produced every year only about 5 % is re-used or sold, usually in production of cement or concrete [16]. That is why there is an ongoing study on ways to try and reuse or dispose FA.

UNIVERSITY of the
WESTERN CAPE

Figure 1.8. Fly Ash dumping.

One of the most studied subjects on ash utilization is the synthesis of Zeolites. FA was found to be the suitable raw material because of its high ratio of Aluminium and Silicon content [4,16], which is the requirement for Zeolites synthesis. Various types of FA Zeolites have been prepared by different methods [4,16,18], these include: Zeolites P, Na-X, Na-A, and Faujasite etc.

1.6. Composite Materials

When two or more materials are mixed together, the resulting composite material very often has physical properties that are very different from the properties of the used composites [19]. The main idea when designing a composite is to take the advantage of the best properties of each component that makes the composite, trying to eliminate their disadvantages, which results in materials with new properties. Composites also occur in nature e.g. a piece of wood is made of long fibres of cellulose (a very complex form of starch) held together by a much weaker substance called lignin [19]. Cellulose is also found in cotton and linen, but it is the binding power of the lignin that makes a piece of timber much stronger than a bundle of cotton fibres. The art of combining different materials to yield new materials with enhanced properties is not a new idea. In most rural areas in Africa the use of mud bricks is common. In order to make these bricks stronger they put a piece of straw or plastics inside the brick, so in that way they combine the tensile (straw or plastic) strength and compressive strength (mud brick). When these bricks are dry and hard, they make a very good building material, which resist squeezing and tearing. Concrete is the well-known composite. Concrete is made of small stones and cement. Cement acts as a binder. Concrete has good strength under compression, and it can be made stronger under tension by adding metal rods, wires, mesh or cables to the composite (so creating reinforced concrete).

UNIVERSITY of the
WESTERN CAPE

There is a large number of different composite materials available today, as for this thesis we had considered two types; organic-inorganic and inorganic-organic composites for our literature survey.

1.6.1. Inorganic-Organic

The inorganic –organic composites represent a class of composites where the inorganic part is matrix/host and the organic is the guest. In this thesis we will focus more on the conducting organic polymers. Examples of these inorganic –organic composites includes intercalation of organic conducting polymers in layered like oxides V_2O_5, layered transitional metal sulphides like Mo_2S_2, chlorides like Rh_2Cl_3, and oxychlorides FeOCl, silicates and phosphates as well as insertion in zeolitic channels [6,8,10]. These composites are formed by initial intercalation of the monomer followed by polymerisation in the inorganic host. Among the inorganic hosts used, clays are the most studied because of their unique layered structure, cation exchangeability and expandability [20]. Clay-PANI is another examples of clay as a host in which PANI emaraldine is produced between the layers of the clay [20,21]. There are two methods to obtain such composites. One can use direct intercalation of a polymer chain into host from solution or molten salt. This method has a disadvantage of slow polymer transport into interlayer space and co-interaction of solvents in case of solution reaction. The preferred method is the intercalation of monomer with subsequent chemical thermal, or photo induced *in situ* polymerisation

UNIVERSITY of the
WESTERN CAPE

1.6.2. Organic-Inorganic

Organic-inorganic composites cater for a very large number of materials with different applications. In our group and in this thesis we concentrated more on conducting organic

polymers as matrix. The organic –inorganic is where the organic is the host and the inorganic is the guest. These guest molecules (inorganic) can be introduced to the host (conducting polymer matrix) in two ways: by covalent linking and by doping [2]. The covalent link results in the formation of metal complexes by introducing the suitable co-coordinating group or molecules. These groups or ligands can be integrated into the polymer chain as a functional group by means of covalent bonds or co-polymerisation with other monomers. Polyaniline (PANI) cannot be used by above method due to the high reactivity of the amino group. The advantage of doping is taken when using PANI. The doping approach introduces the holes or electrons in the polymer chain. This introduction of ionic species as dopants is possible by either ionic exchange or in-situ polymerisation. In this thesis the *in situ* polymerisation approach was used. This approach results in the compounds that are loosely bound having the advantage of simplicity and versatility. In this thesis we will try and make our small contribution to the ongoing research to make the PANI more user friendly. Although many people have done some studies in improvement of PANI by synthesizing nanotubes/rods and fibres, it will be for the first time that FA is used to make nanotubes/rods or even fibres. The thermal stability of PANI composites will also be explored. All these composites will be characterized by different methods to verify the existence of our PANI backbone and Electrochemical Impedance Spectroscopy (EIS) will monitor the behaviour of these materials at low and high frequency. Morphology of these materials will be determined by Scanning Electron Microscopy (SEM).

UNIVERSITY of the
WESTERN CAPE

In Chapter 2 on the basis of our aim of this thesis, our literature review is conducted on polyaniline nanocomposites and nanotubes/rods. Very few literatures are found on PANI-FA composites, as this material is new. Synthesis procedure is presented in Chapter 3, and in Chapter 4 we present the results and discussion. This work is concluded in Chapter 5 where the summary of the overall results is discussed.

UNIVERSITY of the
WESTERN CAPE

CHAPTER 2

LITERATURE REVIEW

2. Introduction

Only one research work is found on Polyaniline –Fly ash composites. Due to the fact that fly ash contains mainly different metal oxides some of which are used to prepare nanocomposites of conducting polymers, the literature survey focused on polyaniline-based nanocomposites.

UNIVERSITY of the
WESTERN CAPE

2.1. Polyaniline-Fly Ash (PANI-FA) composites

Recently the PANI-FA composites were synthesized for the first time, by Raghavhendra *et al*. [1] by *in situ* polymerisation of aniline in the presence of fly ash (FA). These composites were prepared with varying weight percentages. The composites prepared showed decrease in conductivity as the amount of FA increased. The main components of South African FA are; silica (SiO_2), aluminium (Al_2O_3), Calcium oxide (CaO), Iron oxide (Fe_2O_3), MgO and Titanium oxide (TiO_2) [16]. These metal oxides have been used in one way or other in the preparation of nanocomposites or nanotubes/rods. (Al_2O_3) and (Fe_2O_3) have been used as catalyst supporter for the production of nanotubes [3, 4]. Huang [22] has reported that nanotubes can be grown on the silica spheres. The

nanotubes were grown in large curvature of silica surface by pyrolising with iron (II) phthalocynanine

2.2. Polyaniline nanocomposites

Conducting polymer nanocomposites were first synthesized by polymerisation of monomers such as pyrrole, aniline and thiophene in the presence of various metal oxides [8]. These nanocomposites have novel charge storage, magnetic and catalytic properties [21, 22]. Polyaniline has been used to prepare nanocomposites by using clay, transitional metals oxides such as titanium oxide (TiO_2), Cadmium Cd, Vanadium oxide (V_2O_5), tin oxide (SnO_2) [11-14] etc. These nanocomposites can be prepared chemically or electrochemically. The polyaniline transitional metals nanocomposites have introduced these materials into serious application such as electronic devices, nonlinear optical systems photo electrochemical systems. It is believed that the combination of n-type semiconductor of transitional metals and p-type of PANI is responsible for the improvement in the polyaniline photo current values due to the occurrence of excitons dissociation at the interface.

UNIVERSITY of the
WESTERN CAPE

Nanoparticles of PANI can also be synthesized by dispersion polymerisation in the presence of polymeric stabilizer. The stabilizer absorbs onto the PANI nuclei and prevents the PANI particles from aggregation via steric stabilization. Many polymeric stabilizers have been used recently, including poly (styrene sulphonic acid) (PSSA), poly

(vinyl alcohol) (PVA), poly (N-vinyl pyrrolidone), poly (vinyl methyl ether) and methyl-cellulose [6]. PSSA is the most commonly used stabilizer due to its acidity which makes it to be used both as dopant and stabilizer at the same time. Nanoparticles produced with PSSA as a stabilizer has uniform size and also improves the conductivity of PANI [6].

2.3. Polyaniline nanotubes

Nanotubes and nanowires have received much attention since the discovery of carbon nanotubes by Sumio Iijima in 1991[23]. Carbon nanotubes are the first materials to introduce nanotubes to the world of science. Their tensile strength is said to be 100 times more than that of steel, their electrical conductivity match that of copper [24]. Carbon nanotubes have some disadvantages which limit them to some possible applications, these disadvantages include; current synthetic methods are unable to selectively grow sensor-suitable semi-conducting carbon nanotubes, limitation of dopants, fictionalisation or modification for incorporation of specific sensing capabilities can only be performed as post-assembly processes [25]. There are many other types of nanotubes, from various inorganic kinds, such as those made from boron nitride, to organic ones, such as those made from self-assembling cyclic peptides (protein components) or from naturally-occurring heat shock proteins (extracted from bacteria that thrive in extreme environments) [23, 26]. PANI nanotubes are the most preferred because they have properties that are not found in the carbon nanotubes. Nanotubes of polyanilines are not limited to dopants, they are easy to functionalise, and they have electrical, electronic, magnetic, and optical properties similar to metals.

UNIVERSITY of the
WESTERN CAPE

2.3.1. Synthesis

Nanotubes can be prepared chemically or electrochemically using a template or by template free method. When prepared by template, porous materials like Zeolites channels, track-etched polymer membranes, and anodized alumina membranes, or soft templates including surfactants and micelles are used. The desired materials are synthesized within a template, which is dissolved leaving the material in the nanostructure corresponding to shape of the template. The molecular structure and the properties of the nanostructure are determined by the formation mechanism and the template properties [27]. When the template is removed, the polymer nanotubes/ fibres may form undesirable aggregated structures. The most preferred method is the template free method, in this method unlike template synthesis you don't have to remove or dissolve the template after the desired material has been synthesized.. It is called template- free method because a surfactant, which acts as a template or a dopant, is used. Naphthalene Sulphonic Acid (NSA), Camphor Sulphonic Acid (CSA), and Polystyrene Sulphonic Acid (PSSA) has been used [23,25, 28] as dopants and templates, this is termed self assemble template free method.

UNIVERSITY of the
WESTERN CAPE

2.3.2. Formation mechanism of nanotubes

Below is the illustration of the formation mechanism of template-guided synthesis. It can be seen that the shape or size of the product is strongly influenced by the shape and properties of the template as explained above. Li et al [23] used polyacrylic acid as a

template. From the diagram below it can be seen that the nanocomposites formed has a shape of the template and the template need to be removed after the synthesis.

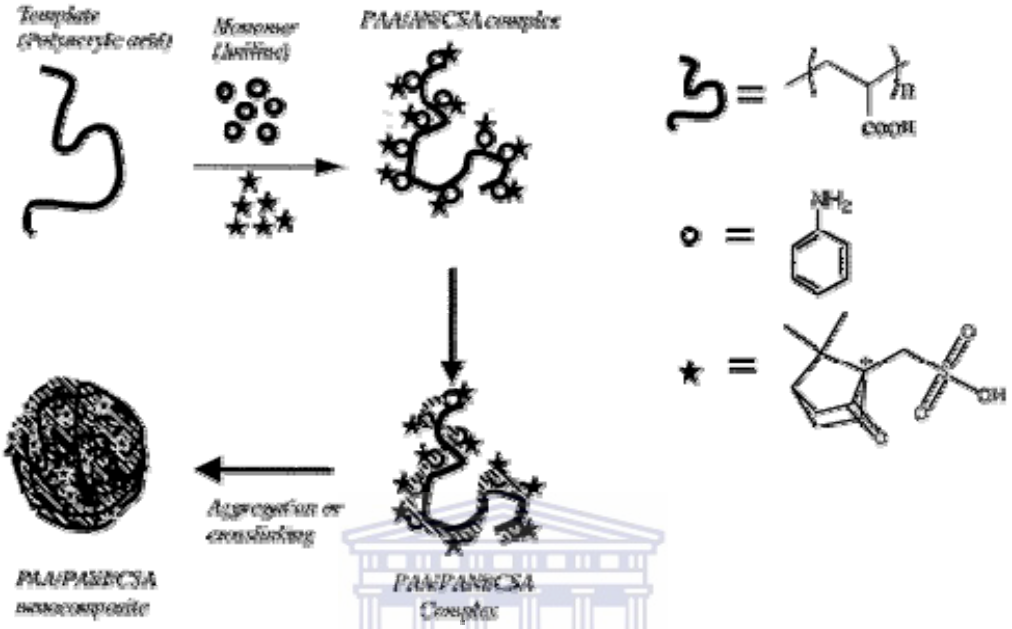

Figure 2.1. Example of a template guided synthesis of nanotubes [23].

UNIVERSITY of the
WESTERN CAPE

The template free method is illustrated below. It must be noted that the morphology and properties of nanotubes produced is strongly affected by the temperature and the concentration of the surfactant or dopant. Whether the tubes or rods are going to be formed is depended on the ratio of aniline to the dopant. In the diagram below Zhang et al [24] proved that nanotubes could be prepared with self-assembly method with or without a surfactant. Micelles A and B are formed in the presence of a surfactant. It must be noted that in micelles B there is excess aniline which is seen inside the micelles B. Surfactant is represented by negative charge and anilinium ions represented by positive. The polymerisation takes place in the water interface because Ammonium per Sulphate (APS)

cannot penetrate the micelles surface. Therefore micelle A will most likely form tubes and micelle B will form rods or fibres. When there is no surfactant, anilinium salt (represented by positive charge) forms micelles, which act as the template. In the figure below micelles C and D represents the micelles formed in the absence of a surfactant. It can be seen that micelles B has excess aniline therefore it will form rods/fibres and micelles C will form tubes.

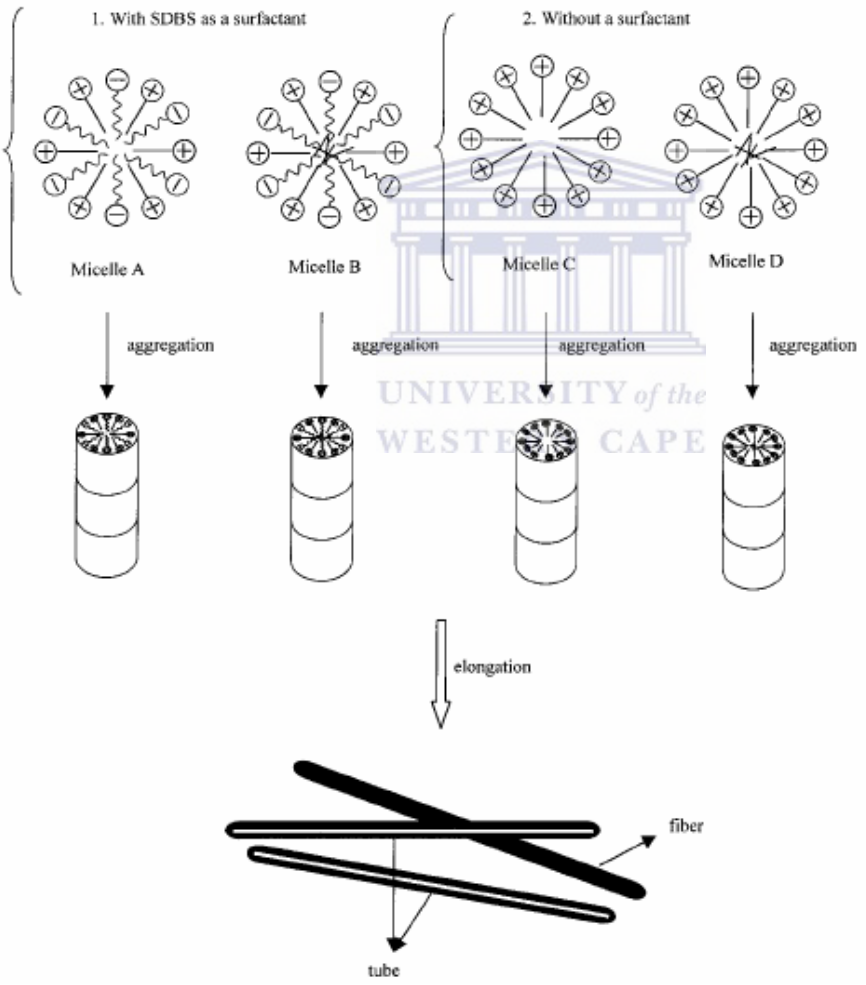

Figure 2.2 Example of template free synthesis of nanotubes/rods [24].

UNIVERSITY of the WESTERN CAPE

According to Zhang et al [28] surfactant is not a prerequisite for nanotubes or rods, which means that any additive that can form micelles (e.g. transitional metals, PSSA etc) can also form nanotubes or rods.

2.4. Electrochemical characterization: background

2.4.1. Cyclic Voltammetry

UNIVERSITY of the
WESTERN CAPE

Of all the electrochemical methods used to characterize PANI, cyclic voltammetry is the most widely used. Cyclic voltammetry consist of measuring the current, which is a result of applied potential. The potential is cycled between a predetermined potential window, from an initial potential E_i to a switch potential E_λ at a constant scan rate. The scan rate can vary from less than 1 mV/s to up to a few thousand mV/s [15, 29]. When a potential is applied on the electrode surface to oxidize or reduce the species in the solution, current arises due to the depletion of species in the vicinity of the electrode. The potential does not stay constant; it rises at a constant rate until it reaches a certain maximum, and decrease back to the initial potential. When the potential is scanned from negative l to positive is said to be oxidizing, and when from positive to negative it is reducing. The cyclic voltammetry can be reversible, irreversible or quasi-reversible [15].

The reversible system is shown in the figure below. Let's consider the following reversible reaction; O +ne=R, with only O initially present in solution. The initial sweep direction will be negative but if we have R, initially present in solution we will have the opposite, the sweep direction will be positive [15]. The observed faradic current depends on the kinetics and transport by diffusion of the electroactive species. So it is necessary to solve the equations, corresponding to Fick's second law for *O* and *R*:

$$\frac{\partial[O]}{\partial t} = Do\frac{d^2[O]}{dx^2} \qquad \ldots(2.1)$$

$$\frac{\partial[O]}{\partial t} = D_R\frac{d^2[R]}{dx^2} \qquad \ldots (2.2)$$

UNIVERSITY of the
WESTERN CAPE

Where [O] is the concentration of oxidant, [R] is the concentration of reductant, D_O is the diffusion coefficient of the oxidant, and D_R is the diffusion coefficient of reductant. The above equations are solved by Laplace transform. They result in equation 2.3 below:

$$I_p = -2.69x10^5 n^{3/2} Co^{\infty} D^{1/2} v^{1/2} \qquad \ldots (2.3)$$

The above equation is called Randles-Sevčik equation where:

I_p = peak current (A cm^{-2})

n = number of electrons

C_O = bulk concentration of oxidant (mol cm^{-3})

D = diffusion coefficient ($cm^2\ s^{-1}$)

v = scan rate (Vs^{-1})

The Randles-Sevčik equation is usually used to calculate the diffusion coefficient. It can be seen that I_p is proportional to square root of scan rate ($v^{1/2}$), plotting Ip vs. $v^{1/2}$ will give a straight line with the slope equal to - $(2.69\times10^5)\ n^{3/2}Co^{\infty}D^{1/2}$.

For a totally reversible system:

1. $\frac{I_p{}^A}{I_p{}^C} = 1$

2. $\Delta Ep = E_p{}^A - E_p{}^C = \frac{59}{n} mV$

3 $E_p - E_{p/2} = \frac{59}{n} mV$

4. $I_p \alpha v^{1/2}$

5. E_p is independent of v.

UNIVERSITY of the
WESTERN CAPE

For a reversible system the rate of electron transport is greater than that of mass transport (Nernstian equilibrium is always maintained) in all potential but for a totally irreversible system the rate of electron transport is insufficient to maintain the Nernstian equilibrium, which results in the reversible peak not seen or very small [15].

The Randles-Sevčik equation changes to:

$$I_p = -(2.69x10^5)n(\alpha_c n\alpha)^{1/2} C_o{}^{\infty} D^{1/2} v^{1/2} \qquad \ldots(2.4)$$

The factor nα is the number of electrons transferred including the rate determining step, and α_c is the transfer coefficient.

The transport of electroactive species form the bulk of the solution to the electrode is not governed by diffusion only, but adsorption of the species on the electrode. When both diffusion and adsorption take place the system becomes complicated. When the adsorbed species is the product a pre-peak will be formed, that is there will be a developing small peak formed before the actual peak expected. If the adsorbed species is the reactant that post peak is formed. There will be a developing peak at the end of the actual peak. In this theses when PANI was polymerised in the presence of FA, when there was 50% FA the post-peak was formed as a results of adsorption.

UNIVERSITY of the
WESTERN CAPE

2.4.2. Electrochemical impedance

Impedance is a measure of the ability of a circuit to resist the flow of electrical current. Electrochemical impedance, like resistance obeys ohms law which define resistant in terms of ratio between voltage *E* and current [30].

$$R = \frac{E}{I} \qquad \ldots(2.5)$$

Where *R* is resistance, *E* is voltage and *I* is current. The use of this equation is limited to only one circuit element, which is the resistor. The resistor follows the ohms law at all

current and voltage, its resistance value is independent of frequency and AC current and voltage signals through a resistor are in phase with each other. With these limitations we cannot use the concept of resistance in a real world because it consists of many complex circuits. The impedance is used because it is not limited by above properties of resistance. Electrochemical impedance is measured by applying AC potential to the electrochemical cell, the results is the AC current containing excitation frequency and its harmonics [15,30]. The current can be analysed as a sum of sinusoidal functions at the same frequency but shifted in phase (see figure below).

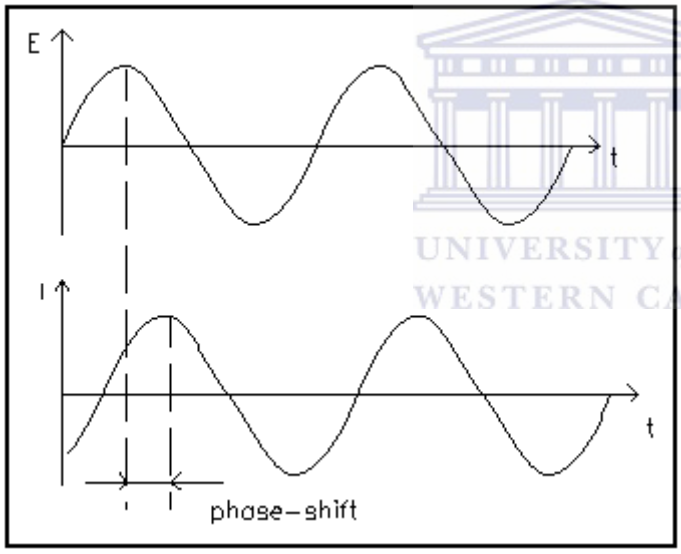

Figure 2.3. Sinusoidal current response.

The excitation signal expressed as a function of time has the form

$$E(t) = E_0 \cos(\omega t) \qquad \ldots (2.6)$$

Where *E (t)* is the potential at time *t*, E_0 is the amplitude of the signal, and ω is the radial frequency. Therefore the relationship between radial frequency (expressed in radians/seconds) and frequency, *f* (hertz) is:

$$\omega = 2\pi f \qquad \ldots (2.7)$$

So current will be represented by

$$I(t) = I_0 \cos(\omega t - \phi) \qquad \ldots (2.8)$$

Where *I(t)* is the current at time *t*, I_0 is the new amplitude shifted by ϕ. By applying Ohms law in calculating impedance we get:

$$Z = \frac{E(t)}{I(t)} = \frac{E_0 \cos(\omega t)}{I_0 \cos(\omega t - \phi)} = Z_0 \frac{\cos(\omega t)}{\cos(\omega t - \phi)} \qquad \ldots (2.9)$$

Euler's cosine Relationship says;

$$e^{(ix)} = \cos(x) + i \sin(x) \qquad \ldots (2.10)$$

Where *i* is an imaginary number, and *x* can be anything. Therefore it is possible to express impedance as a complex function by applying Euler's relationship. The potential can be represented by:

$$E(t) = E_0 e^{(j\omega t)} \qquad \ldots (2.11)$$

and sinusoidal current can be expressed as;

$$I(t) = I_0 e^{(j\omega t - j\phi)} \quad \ldots (2.12)$$

So impedance as a complex function is:

$$Z = \frac{E}{I} = Z_0 \exp(j\phi) = Z_0(\cos\phi + j\sin) \quad \ldots (2.13)$$

Which simplify to:

$$Z(\omega) = Z_{\mathrm{Re}} - jZ_{\mathrm{Im}} \quad \ldots (2.14)$$

UNIVERSITY of the
WESTERN CAPE

Where Z_{Re}, and $Z_{Im,}$ are real and imaginary parts of impedance.

Impedance data can be represented in either Bode or Nyquist plot. In Bode plot, the impedance is plotted with log frequency on the x-axis and both the absolute value of the impedance and phase shift and the phase-shift of the y-axis. The advantage of using the Bode plot is that it shows frequency information; unlike the Nyquist plot where the imaginary (Z_{Im}) part of the impedance is plotted against the real part (Z_{Rel}).

In this thesis we will focus on the Nyquist plot. The advantage of using Nyquist plot is that you can get a lot of information by fitting the circuit with the results. Usually the results come as a semi-circle. The semi-circle is used to fit the equivalent circuit. Below is the typical example of a Nyquist plot. From the picture below it can be noticed that impedance can be represented as a vector with length |Z|. The region of lower frequency is on the right side and higher frequency on the left. The semi-circle below is the example of a single time constant; it is not usually the case, in electrochemical plots often contains several time constants.

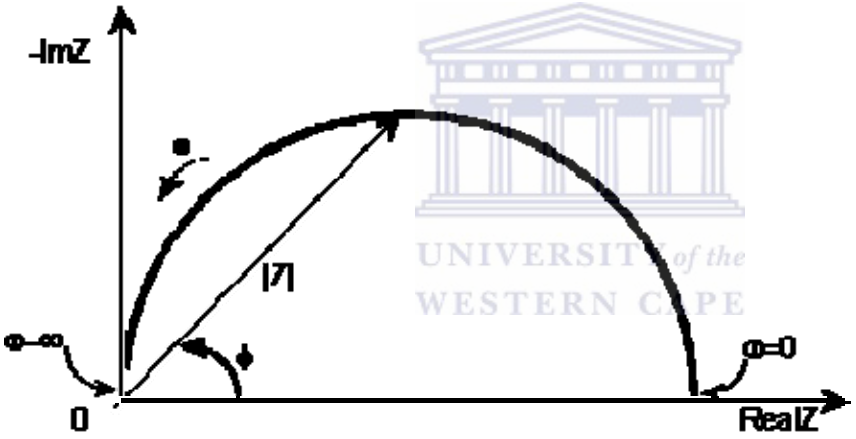

Figure 2.4. Typical Nyquist plot.

Impedance measured by a three-electrode system, where you have a working electrode, reference electrode and counter electrode. The impedance data is fitted to a corresponding circuit with various circuit components. When fitting the impedance data there are two important criteria for identifying the correct equivalent circuit:

1. There must be a good match between the experimental impedance spectrum and the model impedance spectrum over the entire frequency range.
2. Each of the electronic components must be related to one of the parameters of the experimental system.

The circuit elements used to fit the equivalent circuit are explained below.

2.4.2.1 Circuit elements

Solution resistance (Rs)

Solution resistance is the resistance between the working electrode and the reference electrode. The solution resistance is not usually calculated, it is given when fitting the impedance data to a corresponding circuit. The solution resistance (R_s) is found by reading the real value at high frequency intercept [15].

UNIVERSITY of the
WESTERN CAPE

Charge transfer resistance (R_{ct})

Charge transfer resistance (R_{ct}) is another important parameter in impedance, which is kinetically controlled. It is the resistance associated with the charge transfer mechanism for electrode reaction. Charge transfer resistance is the resistance to electrons crossing the interface. It is obtained by reading the real value at low frequency intercept of real values [15].

Capacitor

When ions from the solutions stick to the electrode surface, a double layer is formed in the interface between the electrode and its surrounding electrolyte. This is termed double layer capacitance (C_d). The value of the double layer capacitance depends on many variables including electrode potential, temperature, ionic concentrations, types of ions, oxide layers, electrode roughness, impurity adsorption, ect. The impedance of the pure capacitor is entirely imaginary. It is expressed by this formula:

$$Z_C = (i\omega C)^{-1} \quad \text{…. (2.15)}$$

Where C is capacitance and ω is frequency.

UNIVERSITY of the
WESTERN CAPE

Constant Phase Elements (CPE)

The impedance of CPE is defined by:

$$Z = \frac{1}{[T(Iw)^P]} \quad \text{… (2.16)}$$

Often a CPE is used in a model in place of a capacitor to compensate for non-homogeneity in the system. It is defined by two values, CPE-P and CPE-T were P and T stands for exponent and time constant or capacitance respectively. For example, a rough or porous surface can cause a double-layer capacitance to appear as a constant phase

element with a CPE-P value between 0.9 and 1. In fact, a capacitor is actually a constant phase element - one with a constant phase angle of 90 degrees.

When a CPE is placed in parallel to a resistor, a Cole-Element (depressed semi-circle) is produced.

CPE can be used to describe pure resistor when P=0, $T= R^{-1}$ and pure capacitor when P=1. It can also describe the Warburg impedance when P=0.5 [15].

Warburg Impedance (W)

UNIVERSITY of the
WESTERN CAPE

Diffusion can create impedance known as the Warburg impedance (*W*). This impedance depends on the frequency of the potential perturbation. At high frequencies the Warburg impedance is small since diffusing reactants don't have to move very far. At low frequencies the reactants have to diffuse farther, thereby increasing the Warburg impedance. On a Nyquist plot the infinite Warburg impedance appears as a diagonal line with a slope of 0.5. On a Bode plot, the Warburg impedance exhibits a phase shift of 45°.

2.4.2.2 Equivalents circuits

We have mention all-important parameters needed to fit impedance data into the corresponding circuit. The simplest cell that is usually the starting point for complex fitting is Randles cell. Randal cell has solution resistance, charge transfer resistance and

double layer capacitance. The Nysquist plot of a typical Randles cell is shown below, it is a semi-circle. The solution resistance (R_s) is found by reading the real value at high frequency intercept and the Charge transfer resistance (R_{ct}) is found by reading the real value at low frequency intercept of real values.

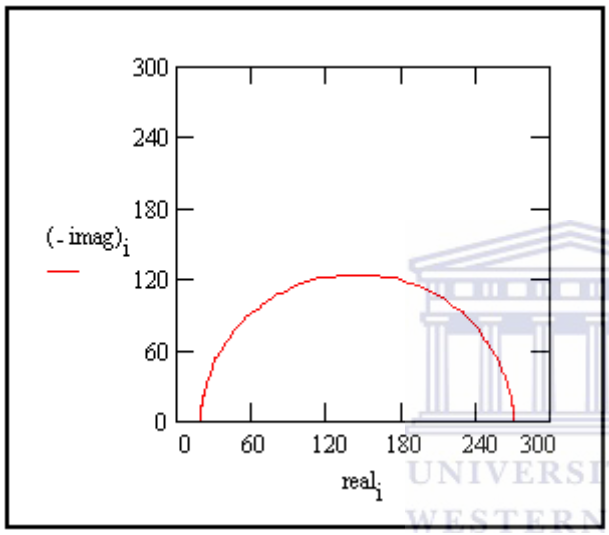

UNIVERSITY of the WESTERN CAPE

Figure 2.5**.** Example of Randles cell's Nysquist plot.

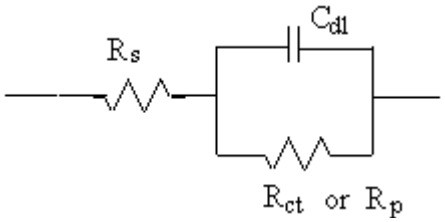

Figure 2.6**.** Equivalent circuit for Randles cell where C_{dl}, R_{ct}, R_p and R_s stands for double layer capacitance, charge transfer resistance, polarisation resistance and solution resistance respectively.

When the polarisation is due to combination of diffusion and kinetic processes, the Nysquist plot is the same as that shown in the figure below. The corresponding circuit is also shown.

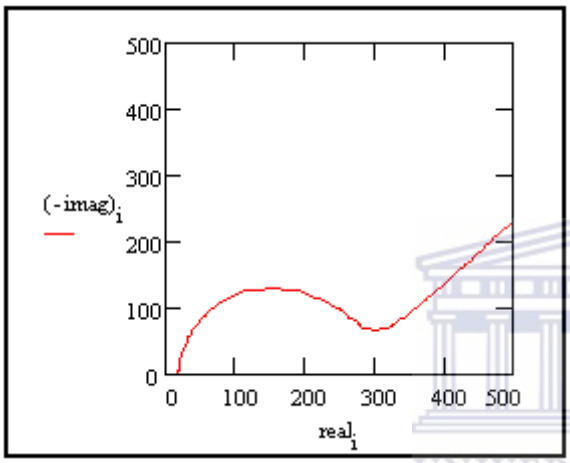

UNIVERSITY of the
WESTERN CAPE

Figure 2.7. Nysquist plot of diffusion controlled system.

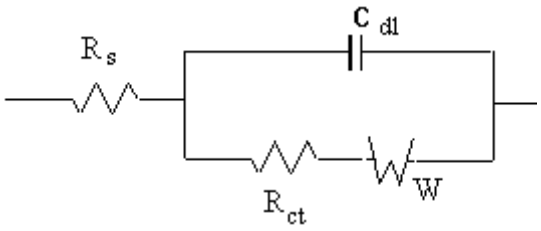

Figure 2.7**.** Equivalent circuit of diffusion controlled system.

The good thing is that there are modern programs to fitting the impedance data into a circuit, one the programs is called Z view2, which is used in this thesis. One of common

use of impedance is to measure corrosion. A good coat usually has very high impedance, it usually a vertical line from a certain at real axis to imaginary axis. Two semi-circles characterize a failed coating. This makes sense because most coatings degrade with time, after certain time water penetrate into coating and forms new water/metal interface.

UNIVERSITY of the
WESTERN CAPE

CHAPTER 3

EXPERIMENTAL

3. Introduction

Details of experimental process and characterization of the PANI-FA composites are presented in this chapter. The method of Raghavendra [4] slightly modified was used for the preparation of PANI-FA composites. Also a modification of the method reported by Cho [5] was used for *in situ* polymerisation of aniline in the presence of FA and the stabilizer PSSA.

UNIVERSITY of the
WESTERN CAPE

3.1 Synthesis procedures

3.1.1 Materials used

Aniline was distilled before use. FA used was collected from Matla Power Station in Mpumalanga province. Aniline, ammonium per sulphate, polystyrene sulphonic acid and hydrochloric acid were used as received and were all purchased from Aldrich.

3.1.2 Synthesis of PANI-FA composites

The method used to prepare PANI-FA was taken from reference [4]. PANI-FA composites with fly ash to aniline ratio (w/w) 20, 30, 40, and 50 % were prepared by *in situ* polymerisation of aniline in the presence of FA.

Aniline (0.1 mol) was added into 1000 mL of 2 M HCl. The solution was stirred and Fly ash was added with vigorous stirring. The mixture was kept in an ice bath with continuous stirring. 0.1 mol of ammonium per sulphate (APS) was added slowly as an oxidant to polymerise aniline. The reaction turned green after some few minutes, which is the indication of the formation of polyaniline in its doped state. The reaction mixture was stirred for 8 hours. The product was collected by filtration and washed by water and acetone until the filtrate was colourless and dried at room temperature.

UNIVERSITY of the
WESTERN CAPE

3.1.3 Synthesis of PANI-FA aged composites.

Here we have slightly modified the above-mentioned method. Aniline (0.1 mol) was added to 1000 ml of 2 M HCl and different percentages of FA were added (as in 3.1.2). The mixture was kept in the furnace for 48 hours at 100 ^{o}C. The mixture was cooled in the ice bath (0-5 ^{o}C) and stirred. After 30 minute 0.1 mol APS was added to the reaction mixture, which was stirred for 5 hours and then kept in the ice bath for another 5 hours. The reaction mixture was removed from the ice bath and kept at the room temperature 12 hours. The product was collected by filtration and washed by water and acetone until the filtrate was colourless and dried at room temperature

3.1.4 Synthesis of PANI-PSSA-FA

In this method we have slightly modified the synthesis technique reported by Cho [5]. We have prepared PANI-PSSA-FA composites by polymerising aniline with FA. PANI-PSSA-FA composites were prepared using same percentages of FA to aniline ratios (w/w) as mentioned before. The amount of PSSA was kept constant in all samples. 10.93 mL of PSSA was dissolved in 555 mL of water and 9.3 mL of HCl and 10.68 mL of aniline were added to the mixture which was kept in an ice bath with continuous stirring. Ammonium per sulphate (13.84g) was dissolved in 80 mL of water; this solution was added slowly to the reaction with continuous stirring on an ice bath for 12 h. The product was collected by filtration and washed with water and acetone. The sample was dried at room temperature.

UNIVERSITY of the
WESTERN CAPE

3.1.5 Synthesis of PANI-PSSA-FA aged.

Here the method is the same as described above except that the reaction was aged before polymerisation of aniline. PSSA was dissolved in distilled water followed by the addition of aniline, HCl and FA. The reaction mixture was kept in furnace for 48 hours at 100^0C. The reaction was cooled in the ice bath. After 30 minutes 13.84 g of APS in 80 mL of distilled water was added and the reaction was stirred for 5 hours and was kept in the ice bath for another 5 hours. The reaction was left at the room temperature for 12 hours. The product was collected as mentioned earlier.

3.2 Characterization

Materials were characterized using the following instruments:

3.2.1 Cyclic Voltammetry (CV)

The BAS/50W integrated automated electrochemical workstation (Bioanalytical Systems, Lafayette, IN, USA) was used for cyclic voltammetry analysis. Pt disk (1.77×10^{-2} cm^2) was used as the working electrode, Platinum wire was used as the counter electrode, and silver wire was used as the reference electrode. The cyclic voltammetry was performed in the 1 M HCl.

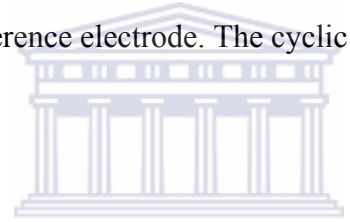

UNIVERSITY of the
WESTERN CAPE

A small amount of composite sample was mixed with 1 M HCl to make a paste. The paste was prepared in such a way as to create the electrolyte environment (not too thick). The three electrodes were dipped into a paste. The CV was performed at the scan rate of 50, 100, 200, 500, 750, and 1000 $mVs^{-1.}$

3.2.2 Electrochemical Impedance Spectroscopy (EIS)

The electrochemical impedance was performed by using Voltalab 80 PGZ 402 Universal Pulse Dynamic EIS (Radiometer Analytical). The three-electrode system was used with the working electrode as Pt disk, counter electrode as Pt wire, and reference electrode as

silver wire. The set up of the cell was the same as that for CV above. EIS was performed at 0 V from 100 MHz to100 kHz and kept at the amplitude of 10 mV.

3.2.3 UV-Vis

The UV-Vis absorbance spectra were recorded at room temperature on UV/VIS 920 spectrometer (GBC Scientific Instruments, Australia) using quartz cuvettes. The composites were dissolved in dimethylfloride (DMF) solution and scanned from 300 to 800 nm.

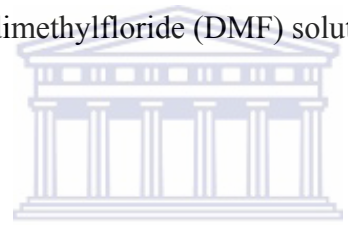

3.2.4. Fourier-Transform Spectroscopy (FT-IR)

UNIVERSITY of the
WESTERN CAPE

The FTIR analysis was done by using a Perkins Elmer, Paragon 1000 PC, in the range of, 4000 to 600 cm^{-1} on KBr pellets. Approximately 15 mg of the sample, plus 1 g of KBr was weighed out, milled and ground in agar mortar and pestle for 5 minutes, until a fine smooth powder of even particle size is obtained. The sample was then transferred into a glass vial. A quarter (~ 0.25 g) of the material and KBr mixture is then pressed with a steel die at 10 $ton.cm^{-2}$ into a pellet.

3.2.5 Scanning Electron Microscope (SEM)

The SEM analysis was done on: Hitachi X-650 Scanning Electron Microscope Operating Voltage between 5-40 kV. A small quantity of sample was dust onto Aluminium stub coated with glue and gold.

3.2.6. Thermal Gravimetric Analysis (TGA)

The TGA was performed by using a Perkin-Elmer TGA 7. The run was carried out from 45 to 900 ^{o}C at a heating rate of 20 ^{o}C min^{-1} in an atmosphere of nitrogen.

UNIVERSITY of the
WESTERN CAPE

CHAPTER 4

RESULTS AND DISCUSION

4. Introduction

The UV-Vis spectra of all samples are presented but for all other characterization only 20 and 40 % fly ash to aniline are taken into consideration. For SEM and TGA we only presented 40 % fly ash to aniline samples.

UNIVERSITY of the
WESTERN CAPE

4.1. FT-IR

The FT-IR was performed for the 40% FA composites because the percentages less than that did not show any differences. The FT-IR spectra of PANI-FA composites are shown in Figure 4.1, while composites that have PSSA are shown in Figure 4.2.

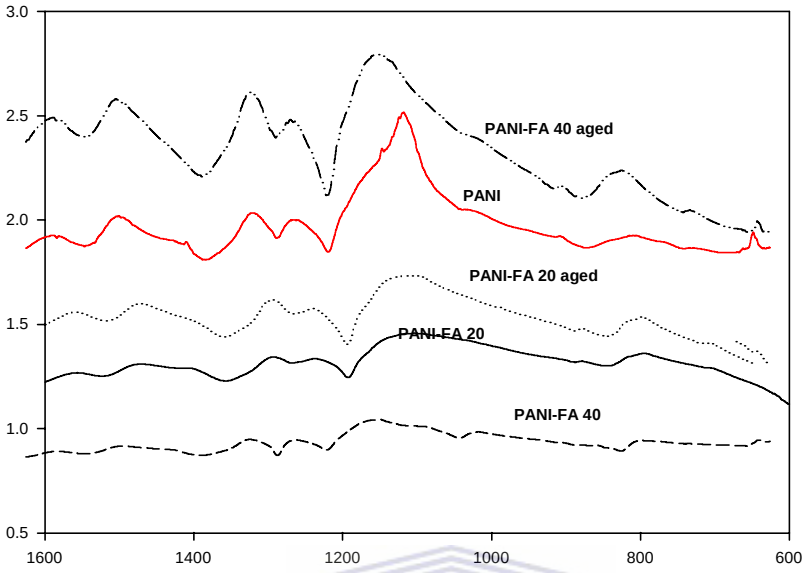

Figure 4.1. FT-IR spectra of PANI-FA composites. The x-axis represents the wavenumber in cm^{-1} and y-axis is the absorbance.

UNIVERSITY of the
WESTERN CAPE

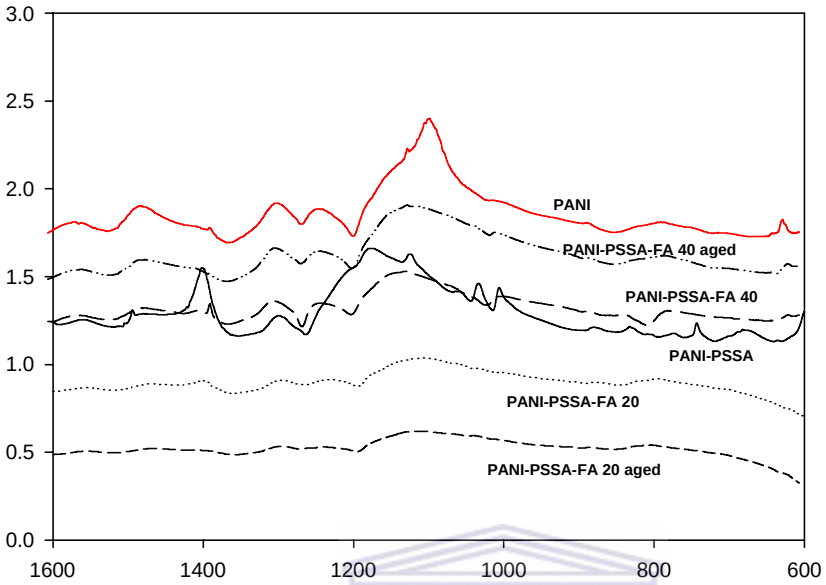

Figure 4.2. FT-IR spectra of PANI-PSSA-FA composites. The x-axis represents wavelength in nm and y-axis represents absorbance.

UNIVERSITY of the
WESTERN CAPE

All composites in both Figure 4.1 and 4.2 show the same peaks around 1558 and 1469 cm^{-1}which are due to stretching vibrations of N=Q=N and N-B-N structure respectively (where =Q= and –B- stands for quinoid and benzonoid moieties in polyaniline backbone) [10,14,31,32]. The positions of these peaks show that the polymer was doped because when polyaniline is undoped these peaks are found between 1590-1600 cm^{-1} for quinoid and 1500-1490 cm^{-1} for benzoic rings [14].

PANI-PSSA in Figure 4.2 has a very sharp peak at 1393 cm^{-1}. This peak is due to C-N stretching of phenyl sulphonic acid substituents [10]. This peak is also observed in PANI-

PSSA-FA composite but is weak, which may be because of physical interaction of FA components with sulphonic acid substituent.

All composites have Peaks at 1296 and 1238 cm^{-1} are observed in all composites in Figure 4.1 and 4.2. These peaks are due to C-N stretching of aromatic rings and C-N stretching of polarons [7,8] respectively. PANI-PSSA has a peak at 1167 cm^{-1}due to $-SO_3H$ [10]. The presence of peaks at 1143-1136 cm^{-1} is the characteristics of conductivity [31,33] since they are described as the measure of charge delocalisation. The FT-IR results show clearly that all the composites have polyaniline backbone, fully doped and conductive.

UNIVERSITY of the
WESTERN CAPE

4.2. UV-Vis results

The UV-Vis spectroscopy of PANI-FA composites and PANI without FA are shown in the Figure 4.3 below.

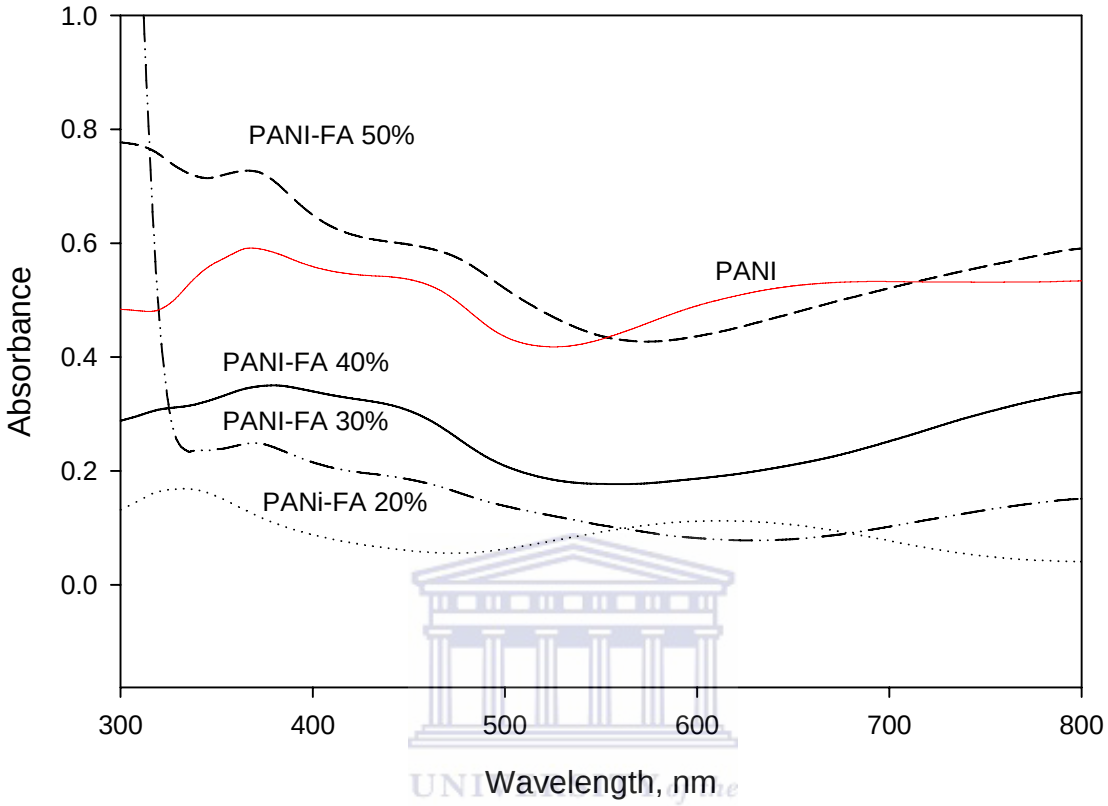

Figure 4.3. UV-Vis Spectra of different percentages of PANI-FA composites

UV-Vis spectra of PANI showed three peaks which at 360, 450 and a broad peak at 550-800 nm, which are characteristic of emaraldine salt [3,26]. The peak at 360 nm is due to $\pi - \pi^*$ of benzoic rings, 450 nm is due to $n - \pi^*$ which is due to polarons band, and 550-800 nm is due to $\pi - n$ which is as a result of excitons and doping level [3,26].

In the case of PANI-FA 20(20% of FA to aniline (w/w) ratio) the peak at 450 nm became very weak and 550-800 nm disappeared, a new peak around 600 nm is formed. The peak

at 360 nm is shifted to 330 nm, which is the indication that PANI changed from emaraldine salt to partially oxidized PANI because of the presence of weak absorption at 450 nm.

In case of PANI- FA 30(30% of FA to aniline (w/w) ratio), PANI-FA 40(40% of FA to aniline (w/w) ratio), and PANI-FA 50 the 330 nm peak is shifted back to 360 nm and the peak at 450 nm became more intense with increase of FA in composites. The peak at 450 nm is due to the polarons [3, 5,14,26], the peak at 550-800 nm reappeared; this peak became broader as the amount of FA increased. This broadness shifted to the lower wavelength as the percentage of FA increases, this means as percentage of FA increases PANI is becoming more doped. These peaks are characteristics of emaraldine salt form of PANI.

UNIVERSITY of the
WESTERN CAPE

The UV-Vis results of composites prepared by ageing method are presented in Figure 4.4.

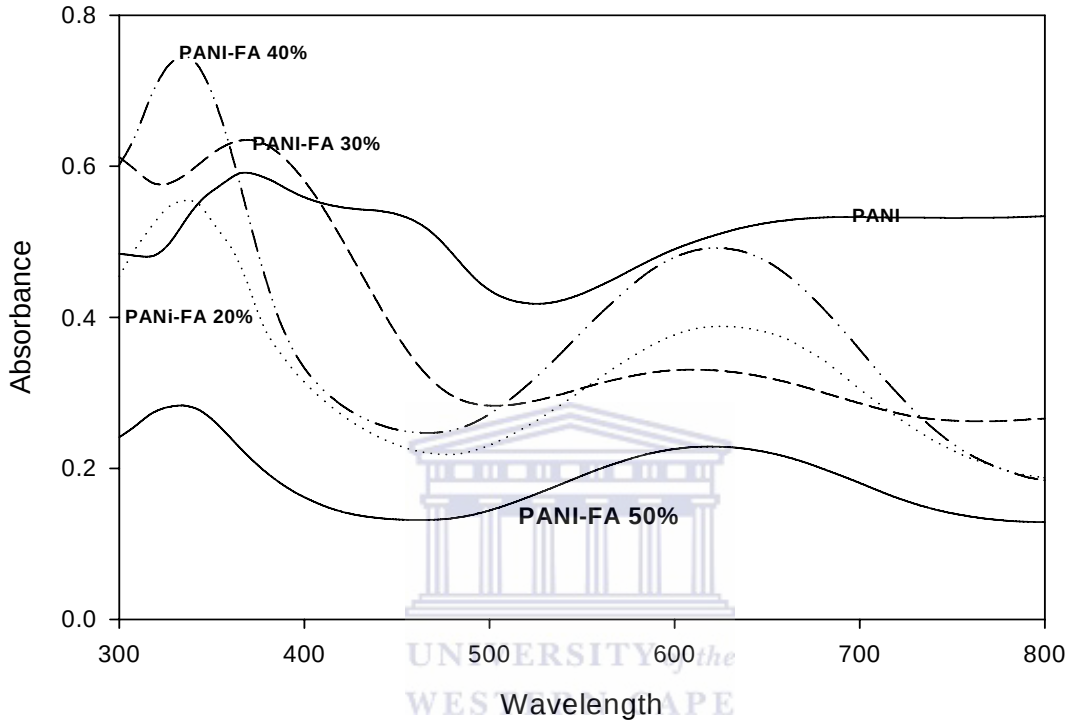

Figure 4.4. UV-Vis spectra of PANI-FA aged composites

In Figure 4.4 the aged PANI-FA composites show two very distinct peaks at 330 and 630 nm. Aged PANI-FA 40 and aged PANI-FA 50 show very weak peak at 450 nm. The presence of this peak indicates that these composites are partially oxidized. The two peaks at 330 and 630 nm are characteristic of emaraldine base. The peak at 330 nm is due to $\pi - \pi^*$ transition of benzoic rings while peak at 630 nm is due to $\pi - \pi^*$ transition of quinoid rings [14,26].

UV-Vis of PANI-PSSA-FA is shown below. PANI-PSSA-FA 20 and 40 show the characteristics of partially oxidized PANI states with three peaks at 330, 450, and 630 nm.. The other composites (PANI-PSSA-FA 30 and PANI-PSSA-FA 50) have characteristics of emaraldine salt, with peaks at 360 nm, 450 nm and broad peak starting at 700 nm. The position of the peak of PANI-PSSA is shifted to the higher wavelength at 385 nm as compared to other emaraldine salts for which the peak is around 360 nm. These shifts indicate increased conductivity. These results are comparable with those observed by Cho [5] when he polymerises aniline in the presence of PSSA

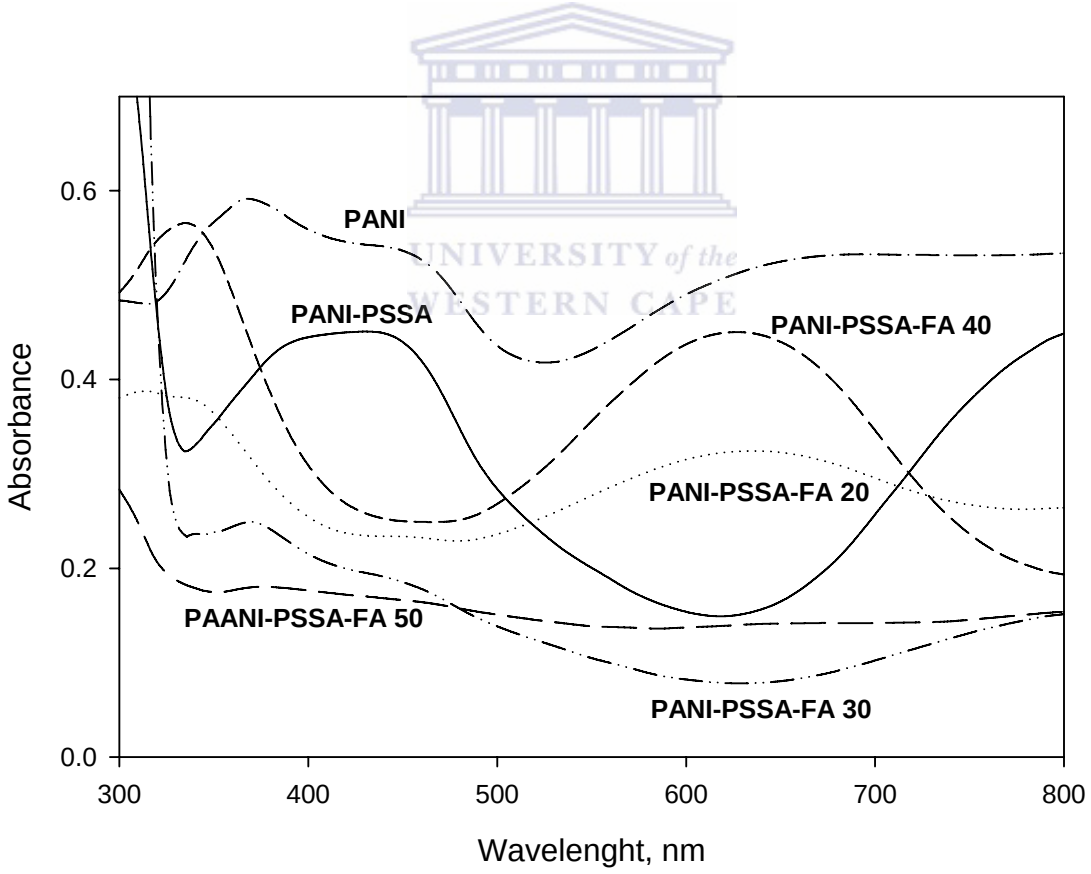

Figure 4.5 UV-Vis spectra of PANI-PSSA-FA at different FA%.

UNIVERSITY of the WESTERN CAPE

The UV-Vis spectra of PANI-PSSA-FA aged composites are shown in the Figure 4.5 below. All composites have peaks at 330, 450, and 630 nm. It seemed as if the presents of FA lowers the wavelength therefore increasing the band gab energy and decreasing the conjugation.

.

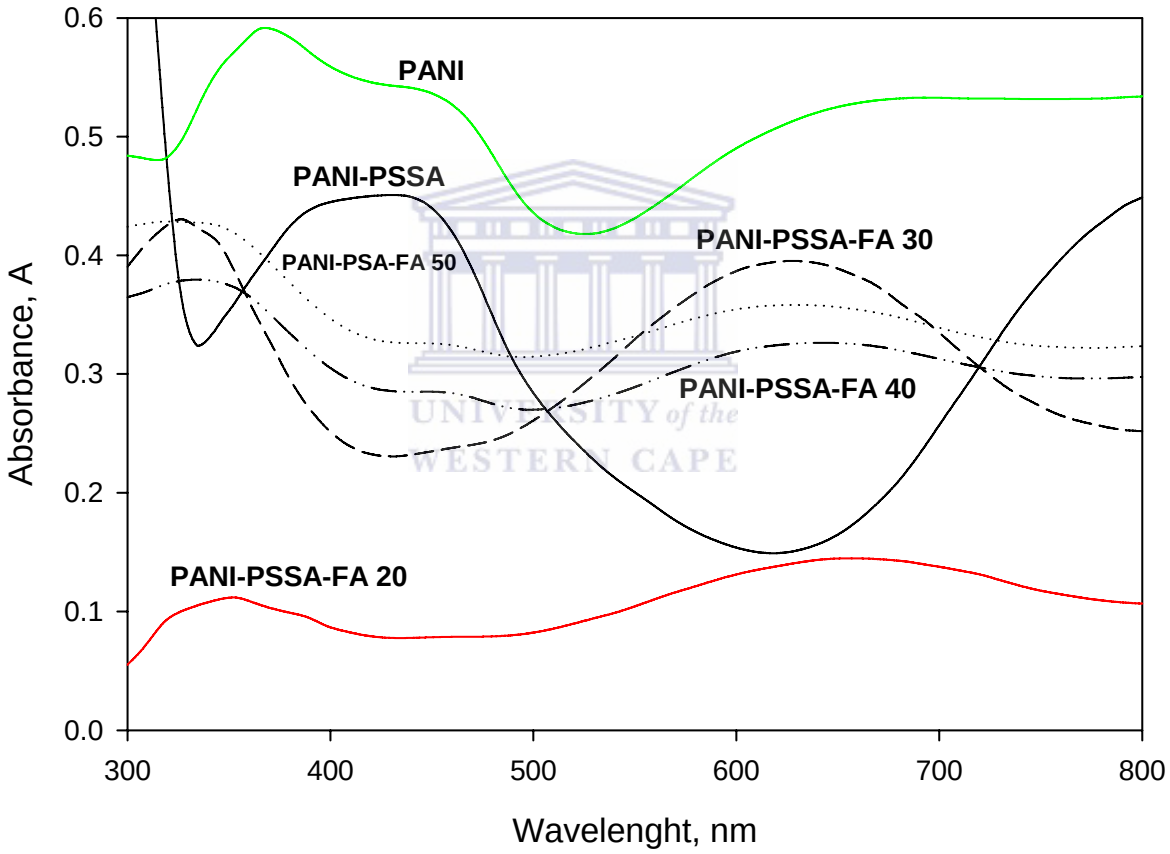

Figure 4.6. UV-Vis spectra of PANI-PSSA-FA aged

4.4. Cyclic Voltammetry (CV)

Cyclic Voltammetry experiments were performed at 100, 200, 500, 750, and 1000 mVs^{-1}

4.4.1. PANI-FA composites

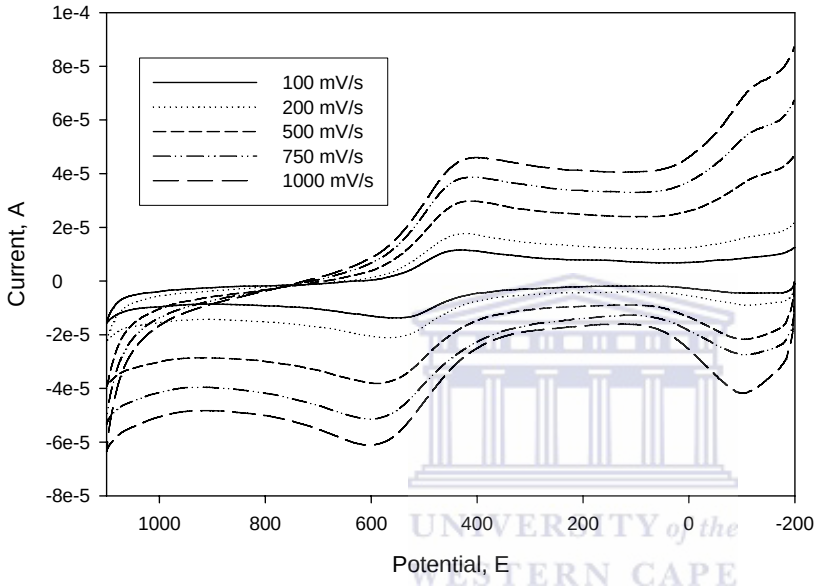

UNIVERSITY of the WESTERN CAPE

Figure 4.7. Cyclic Voltammetry of PANI at different scan rates.

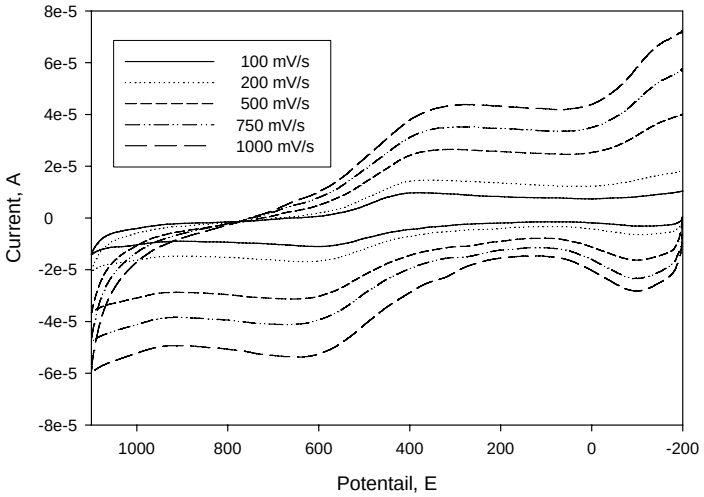

Figure 4.8. Cyclic Voltammetry of PANI-FA 20 at different scan rates.

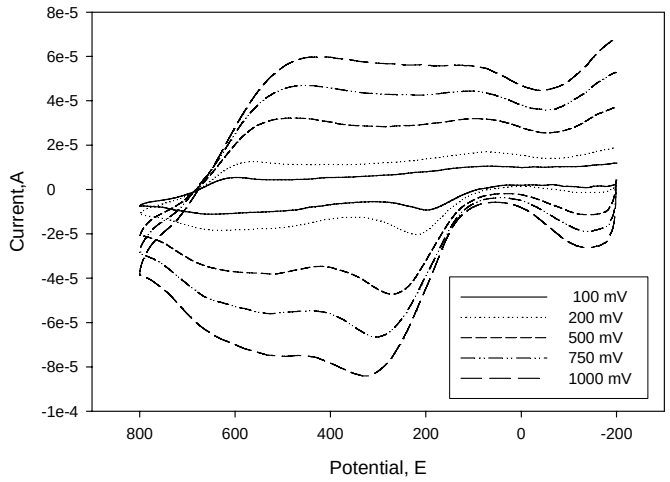

Figure 4.9. Cyclic Voltammetry of PANI-FA 20 aged at different scan rates

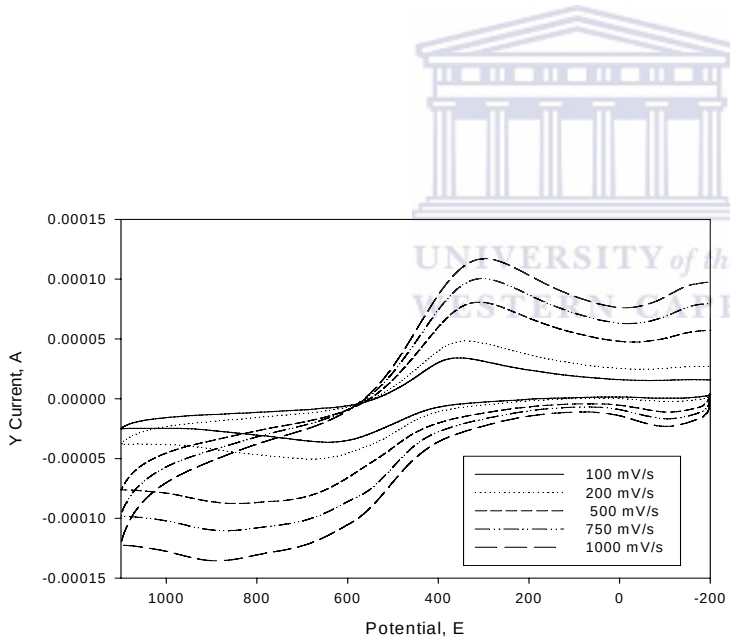

Figure 4.10**.** Cyclic Voltammetry of PANI-FA 40 at different scan rates

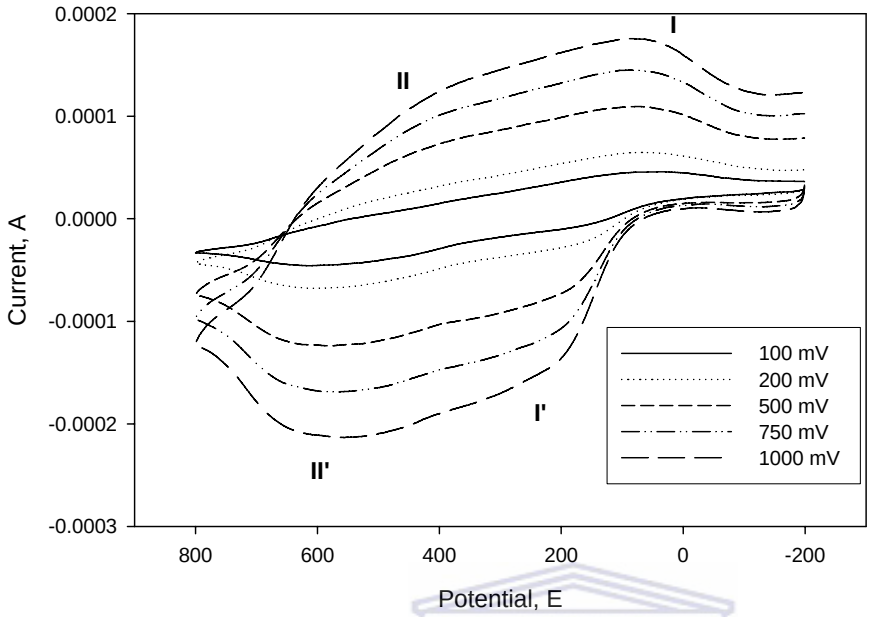

Figure 4.11. Cyclic Voltammetry of PANI-FA 40 aged at different scan rates

UNIVERSITY of the
WESTERN CAPE

The voltammograms (Figure 4.7-4.11) above all show reversibility. The peak current increases with the scan rate and it can be seen that all the peaks are shifting to higher potential as the scan rate is increased. This shows that the composites are electroactive and diffusion controlled [29]. The fact that the scan rate increases with current means that, the polymer is conducting. The shifting means that the charge is moving along the polymer backbone [29].

The CV of PANI and PANI-FA (Figure 4.7, 4.8 and 4.10) shows one anode peak and one cathode peak. It must be noted that PANI synthesized electrochemically shows two reversible peaks, so the results of the CV is dependent on the preparation method. The

two peaks (I and I') observed in Figure 4.7 are due to the transition from fully reduced leucoemaraldine to fully oxidized pernigraniline.

When 20 % FA (Figure 4.8) is added no significant change is observed. The two peaks are also observed here. But as the amount of FA increases as seen in PANI-FA 40 (Figure 4.10) the small post peak develops at the end of peak I. This shows that the reactions involved are governed by diffusion and adsorption of reactants (FA) and FA is adsorbed in the PANI. This is an indication that that FA does not react completely with PANI, there is unreacted FA in the polymer.

For the aged PANI-FA composites (Figure 4.9 and 4.11) two reversible peaks are observed. These peaks can be attributed to the transition of fully reduced leucoemaraldine to half oxidized emaraldine (I/I') and fully oxidized pernigraniline to half reduced emaraldine (II/II')[29,]. Aged PANI-FA 40 in Figure 4.11 has very broad oxidation and reduction peaks. This suggests slow electron transfer. Again a small post peak is observed at oxidation side in the aged PANI-FA 40 (Figure 4.11) it shows that the reaction is governed by both diffusion and adsorption. .

UNIVERSITY of the
WESTERN CAPE

4.4.2. PANI-PSSA-FA composites

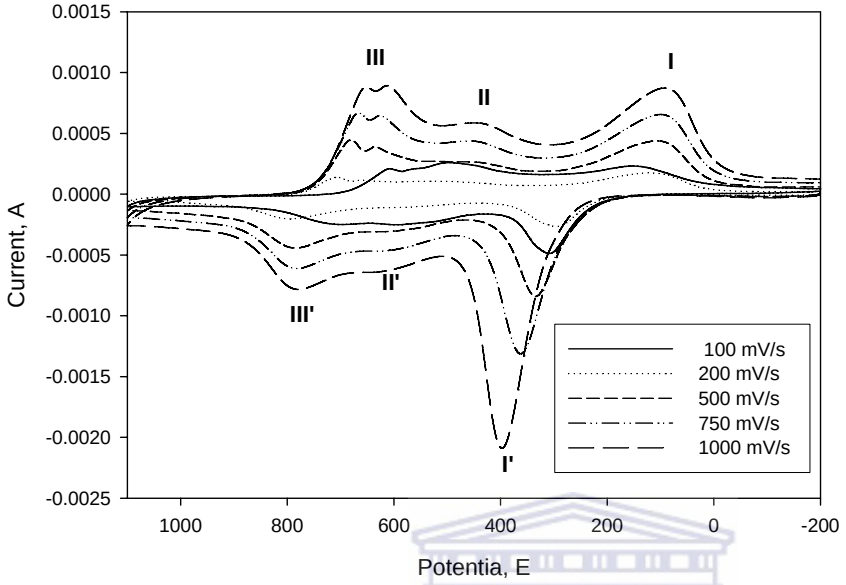

Figure 4.12 Cyclic Voltammetry of PANI-PSSA at different scan rates.

UNIVERSITY of the
WESTERN CAPE

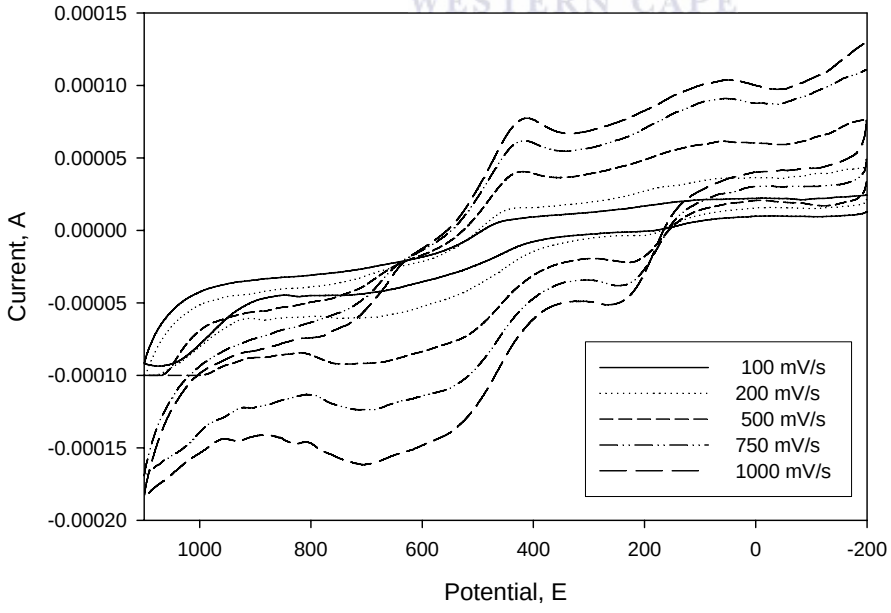

Figure 4.13. Cyclic Voltammetry of PANI-PSSA-FA 20 at different scan rates

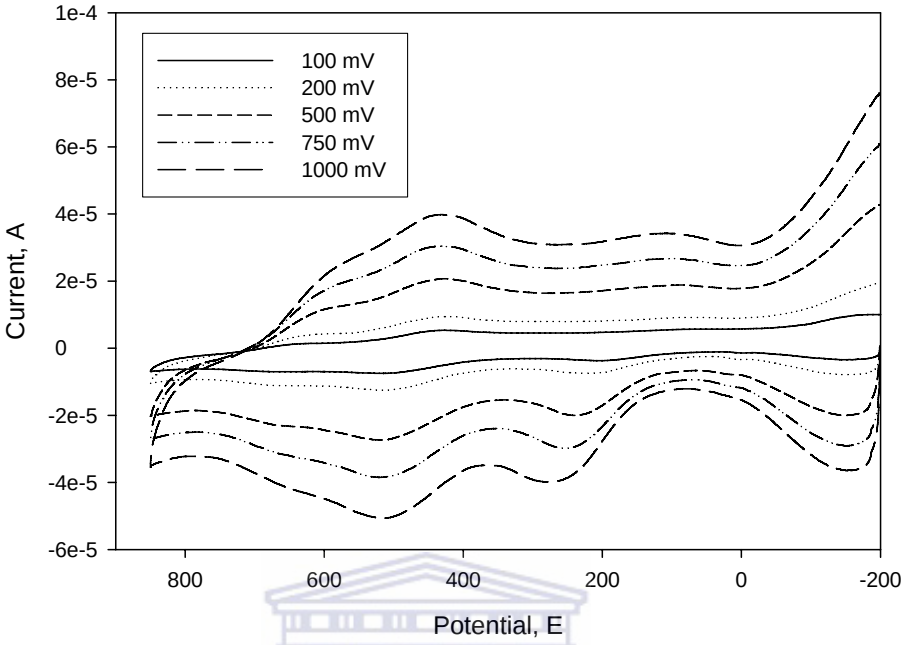

Figure 4.14**.** Cyclic Voltammetry of PANI-PSSA-FA 20 aged at different scan rates

UNIVERSITY of the
WESTERN CAPE

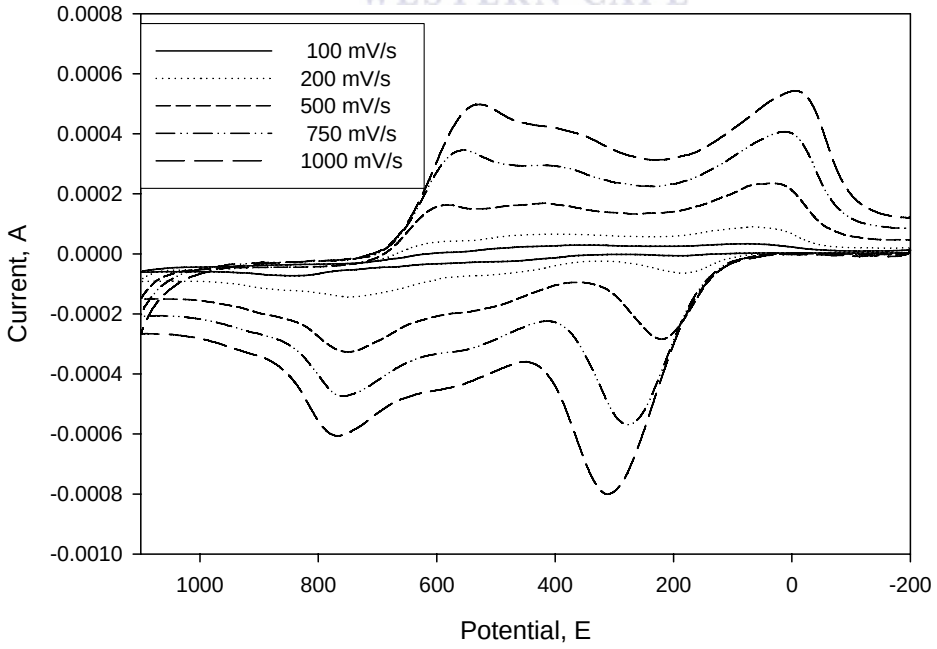

Figure 4.15. Cyclic Voltammetry of PANI-PSSA-FA 40 at different scan rates

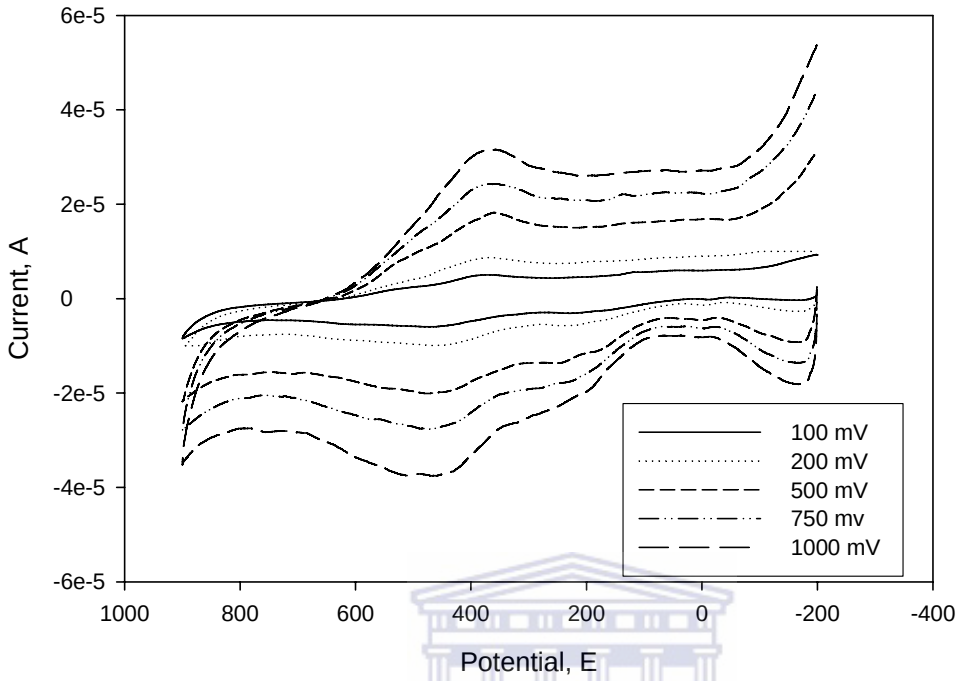

Figure 4.16. Cyclic Voltammetry of PANI-PSSA-FA 40 aged at different scan rates

UNIVERSITY of the
WESTERN CAPE

All the graphs show that the composites are electroactive, conductive and diffusion controlled as discussed above. PANI-PSSA (Figure 4.12) and PANI-PSSA-FA 40 (Figure 4.15) show three peaks, which are characteristics of sulphonated PANI. The middle peak in Figure 4.12 and 4.15 is attributed to either the presence of ortho-coupled polymers or degradation of PANI (soluble species such as benzoquinone and hydroquinone)[37]. The other peaks are attributed to the transition of leucoemaraldine to pernigraniline as discussed above.

When PANI-PSSA-FA composites are aged in Figure 4.14 and 4.16, the first oxidation peak becomes broad. This implies that the electron transfer is slow in the aged composites. It becomes more apparent as the amount of FA increases, as it can be noticed

from aged PANI-PSSA-FA 40 (Figure 4.16) that the first oxidation peak is so broad that it became more flat. The same can be observed in non-aged composites. If we compare the first oxidation peak of PANI-PSSA and that when FA is added, it can be seen that it becomes broader as the amount of FA increases. We can conclude that the presence of FA slows the rate of electron transfer.

The pernigraniline is the most stable form of PANI-PSSA-FA aged. This is in agreement with the UV-Vis data above. If one looks at all the CVs (Both PANI-FA and PANI-PSSA-FA) of composites there is at least one peak (peak I), which does not change the potential but increase only in current as the scan rate is increased. This shows that adsorption takes place and the fact that the current is increasing with the scan rate means that the materials are conductive.

UNIVERSITY of the
WESTERN CAPE

When comparing the voltammograms of PANI-FA and PANI-PSSA-FA composites, the latter does not show any adsorption as compared to PANI-FA

4.4.3 Analysis

As discussed above in 4.4.1 and 4.4.2 the cyclic voltammograms showed that the materials were reversible, diffusion and adsorption controlled.

The rate of diffusion is the amount of the material impinging on the electrode surface per unit time [15,30]. The diffusion constant (De) is a measure of the velocity of electro-analyte as it diffuses through solution prior to electron transfer reaction.

Randles-Sevcik equation is used to obtain the diffusion coefficient (De). For a reversible system the Randles equation is:

$$Ip = 2.69x10^{5} AC^{*} n^{3/2} D^{1/2} v^{1/2}$$

Where Ip = peak current

n = number of electrons exchanged per molecule

A= area of the electrode (m^2)

D = diffusion coefficient (m^2s^{-1})

C^* = bulk concentration ($molL^{-1}$)

v = potential scan rate (Vs^{-1})

UNIVERSITY of the
WESTERN CAPE

Randles-Sevcik of plot anodic peak of PANI from a CV is shown in Figure 4.17 below. According to the equation a plot is suppose to pass through the origin but this is not the case in these materials. The Randles-Sevcik plot assumes that diffusion is the only means of mass transport. The reason for the deviation of Randles-Sevcik behaviour is due to changing current. Another reason is that the exponent in the scan rate is not ½, but other fraction. If the exponent is grater than half it means that we should assume that other means of mass transport supplement diffusion. If the exponent is less that half, it means that the analyte is adsorbed on the electrode [15,30]. From our CV results we concluded

that adsorption is also involved in the mass transport. This is in agreement with Randles-Sevcik plot where the line does not pass through the origin.

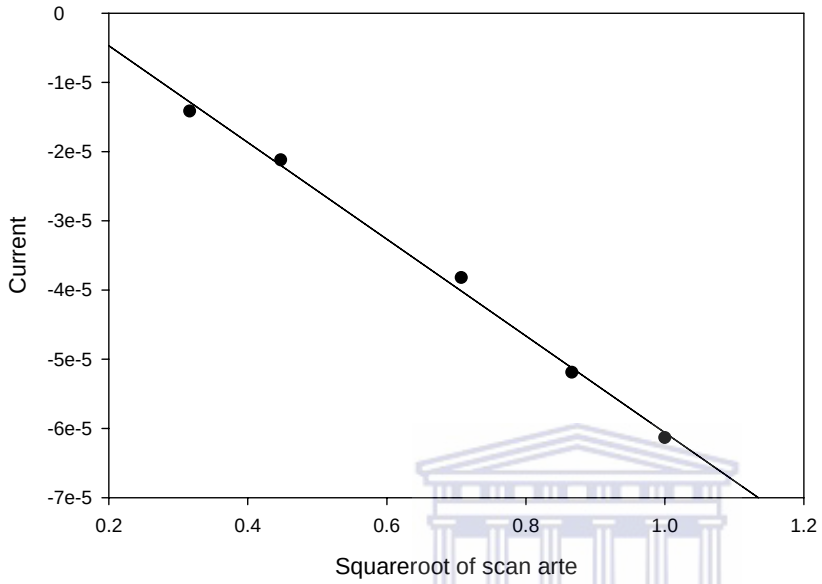

Figure 4.17. Randles-Sevcik plot of PANI

UNIVERSITY of the
WESTERN CAPE

The plot of Ip Vs $v^{1/2}$ will give the slope = $Slope = 2.69x10^5 AC * n^{3/2} D^{1/2}$

The number of electrons exchanged (n) can be obtained by using Tafel plot. The Tafel equation is as follows:

$$In_i = In_{i_0} - \frac{\alpha \eta F n}{RT}$$

The plot of In_i vs ŋ will give a straight line with y intercept = In_{i_0}

Slope = $-\frac{\alpha nF}{RT}$

Where i = current

I_o= exchange current

ŋ = over potential (E-E^o)

F= Faraday constant

T= absolute temperature

The number of electrons exchanged (n) can be calculated using the slope of the Tafel plot.

From the Tafel plot below, the slope of the graph is; -25.79

Therefore -25.79= $-\frac{\alpha nF}{RT}$

UNIVERSITY of the
WESTERN CAPE

-25.79= 0.5x 96500xn/(298x8.314)

n = 1.32

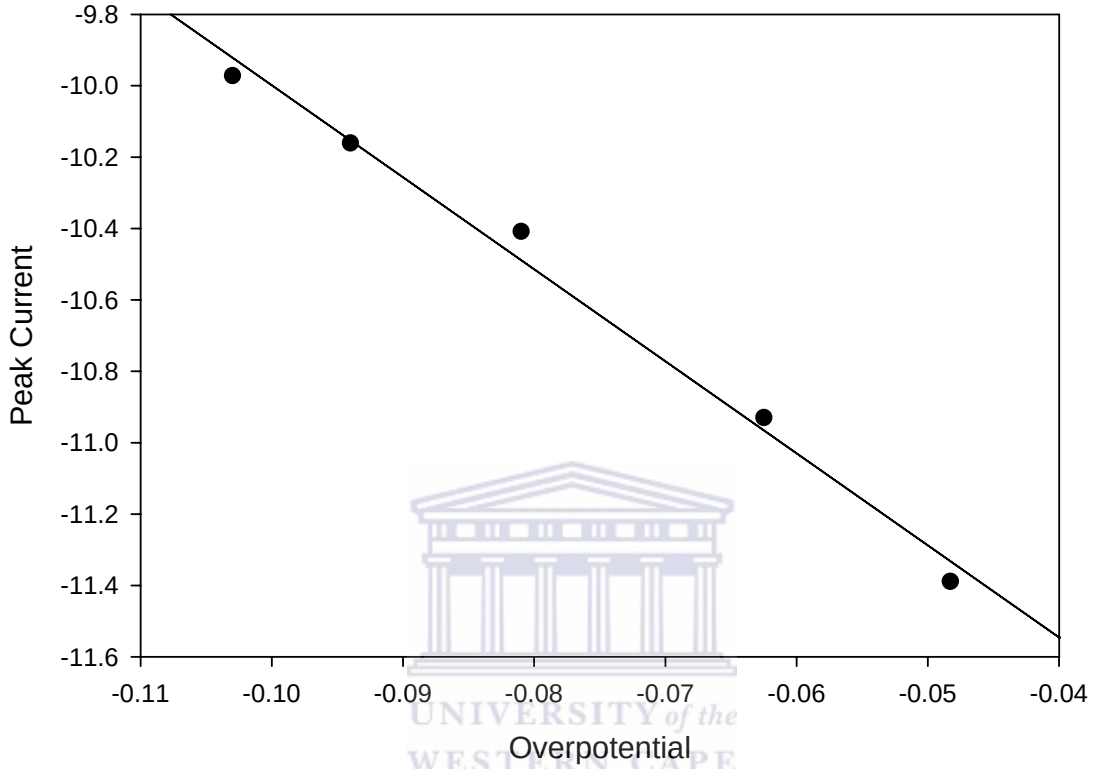

UNIVERSITY of the
WESTERN CAPE

Figure 4.18**.** Tafel Plot of PANI

Diffusion coefficient (D) of PANI can now be calculated easy because we have obtained the number of electrons exchanged (n) from Tafel plot. The slope of Randles-Sevcik plot will help us get D.

$$\text{Slope} = 2.69x10^5 AC_{ox}n^{3/2}D^{1/2}$$

$$-6.9854855693e\text{-}5 = 2.69 \times 10^{5} \times 0.0177 \times 10^{-4} \times 0.1 \times 1\ D^{1/2}$$

$$D = (-6.9854855693e\text{-}5 \times 21)^{2} = 2.148 \times 10^{-6}\ m^{2}s^{-1}$$

The standard rate constant (k^0) can be calculated using the Nicholson and Shaire working curve [29]. The peak-to-peak separation ΔEp is plotted as a function of o Ψ. The parameter Ψ is found from:

$$\Psi = \frac{k^0}{(\alpha nFD/RT)}$$

Where k^0 is the standard rate constant, α, n is number of electrons, *v* is the scan rate, D diffusion coefficient, R is gas constant, and K is absolute temperature. Below the working curve is plotted from the data from Nicholson and colleagues (1965)[29].

UNIVERSITY of the
WESTERN CAPE

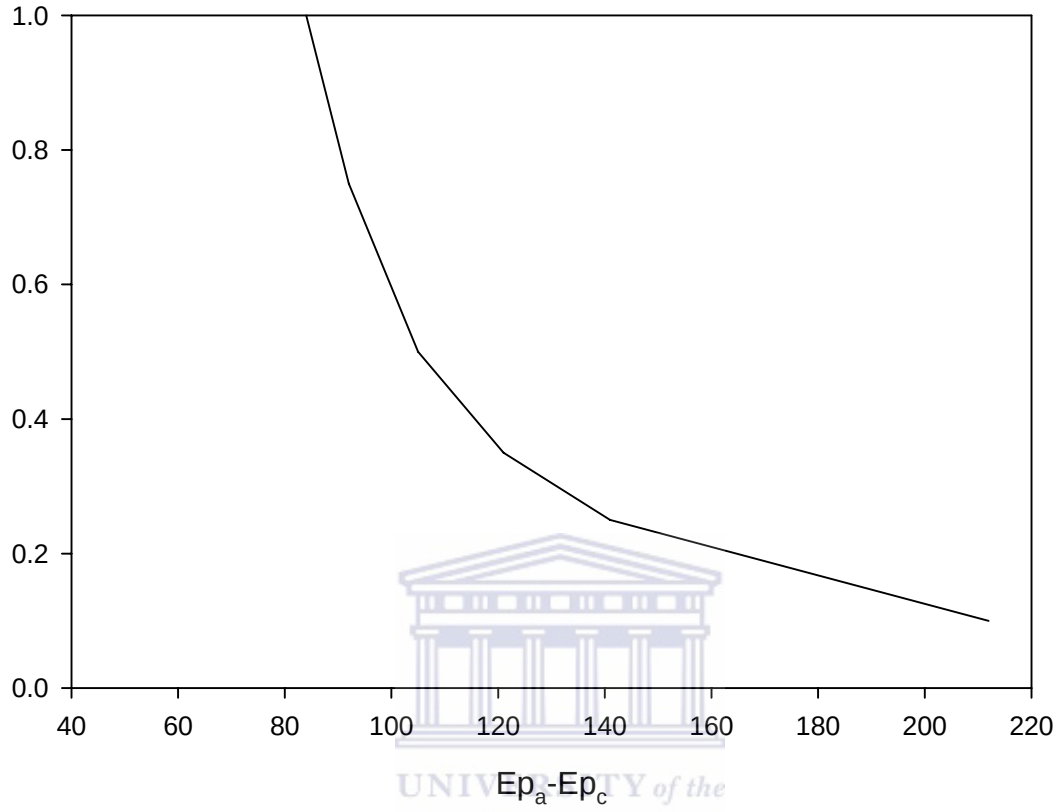

UNIVERSITY of the
WESTERN CAPE

Figure 4.19. Working curve used to calculate ΔEp.

From the PANI CV it was found that ΔEp was 147 mV at 200 mVs^{-1} scan rate, this value correspond to Ψ =0.333

Substituting from the following formula: $\Psi = \frac{k^0}{(\alpha nFD/RT)}$

After substitution k^0 was found to be 8.677 x 10^{-4} ms^{-1}

Table 1. Kinetic parameters

Sample	**Diffusion coefficient (D) $m^2\ s^{-1}$**	**Standard rate constant (k^0) $m\ s^{-1}$**
PANI	2.15×10^{-6}	6.64×10^{-4}
PANI-FA 20	1.61×10^{-6}	1.84×10^{-4}
PANI-FA 40	7.68×10^{-6}	1.94×10^{-4}
PANI-FA 20 aged	5.14×10^{-6}	1.03×10^{-3}
PANI-FA 40 aged	1.84×10^{-5}	3.53×10^{-3}
PANI-PSSA	7.03×10^{-4}	1.02×10^{-2}
PANI-PSSA-FA 20	8.66×10^{-7}	5.95×10^{-4}
PANI-PSSA-FA 40	8.69×10^{-6}	2.15×10^{-3}
PANI-PSSA-FA 20 aged	3.37×10^{-7}	5.64×10^{-4}
PANI-PSSA-FA 40 aged	1.28×10^{-7}	1.41×10^{-4}

UNIVERSITY of the
WESTERN CAPE

Table 1 above shows the kinetic parameters k^0 (standard rate constant) and D (diffusion coefficient). The material with high diffusion coefficient is the one with a rapid electron transfer. The standard rate constant (k^0) measures the intrinsic ability of a species to exchange electrons with the electrode in order to convert to its redox partner. A species

with large k^0 will convert to its redox partner on a short time scale; a species with smaller k^0 will convert to its redox partner on a longer time scale.

Usually the largest values of k^0, characterize redox processes that do not involve significant molecular reorganization (reversible). It must be taken into account that one of the most important factors, which contribute to enhancement of the activation barrier of reorganization, which accompanied the electron transfer.

4.5. Electrochemical Impedance spectroscopy (EIS)

UNIVERSITY of the
WESTERN CAPE

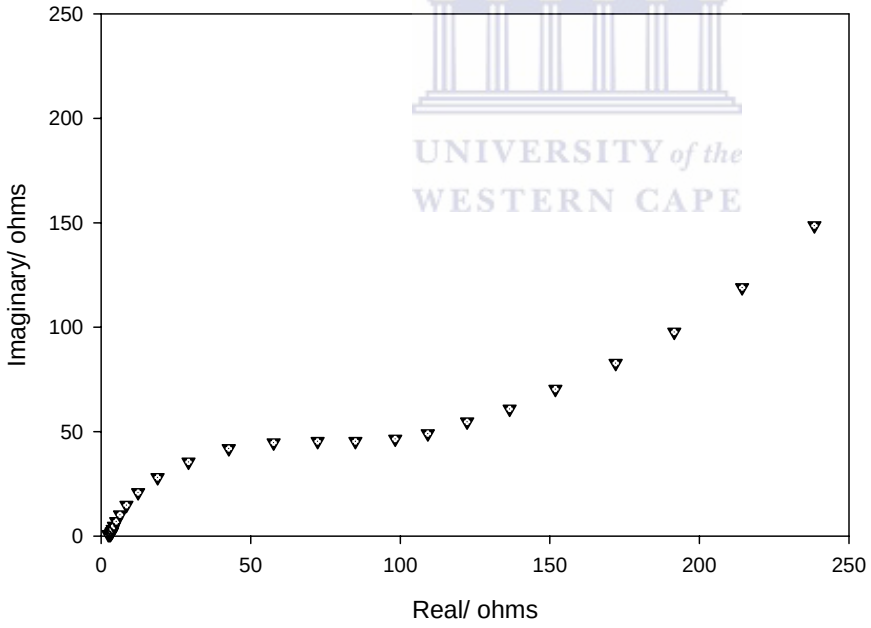

Figure 4.20**.** Impedance spectroscopy of PANI

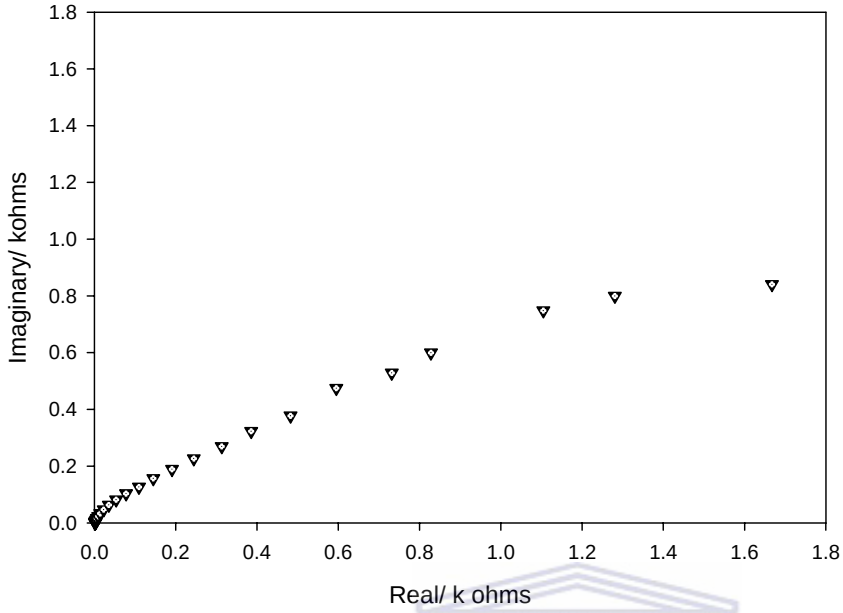

Figure 4.21. Impedance spectroscopy of PANI-FA

UNIVERSITY of the
WESTERN CAPE

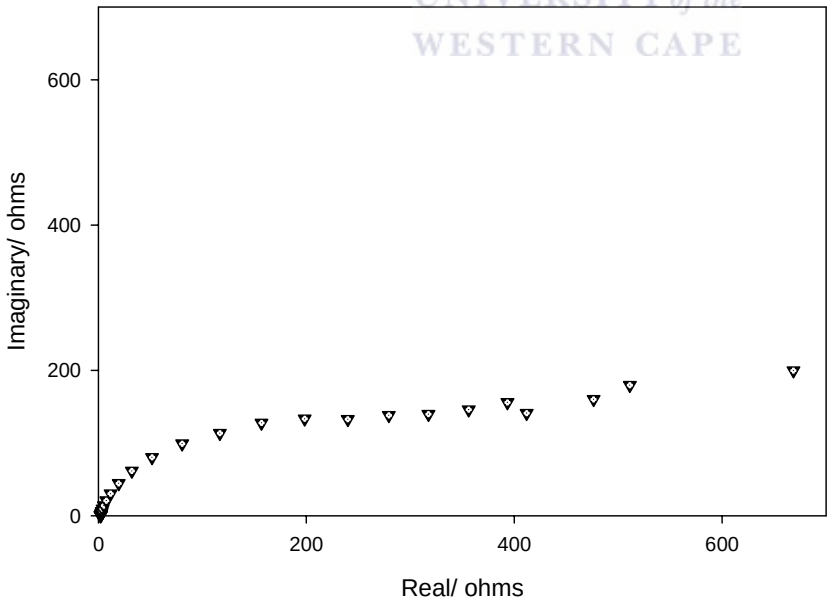

Figure 4.22. Impedance spectroscopy of PANI-FA aged

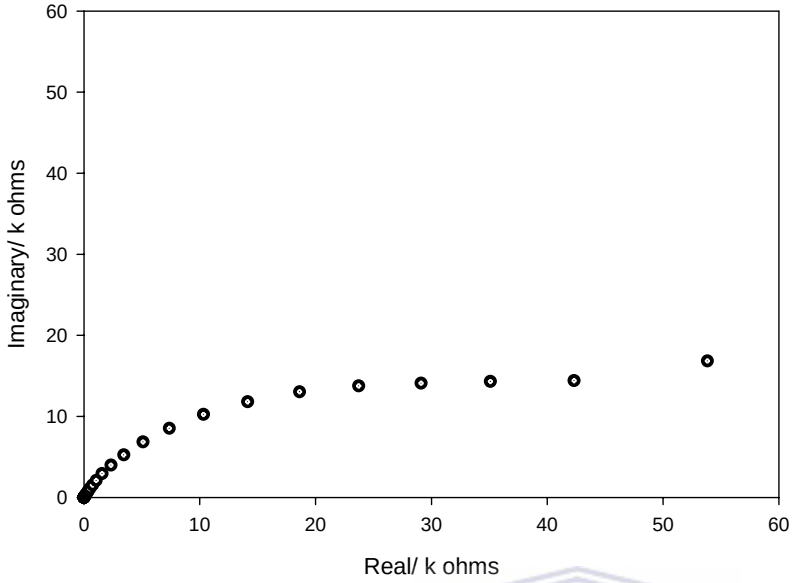

Figure 4.23. Impedance spectroscopy of PANI-PSSA

UNIVERSITY of the
WESTERN CAPE

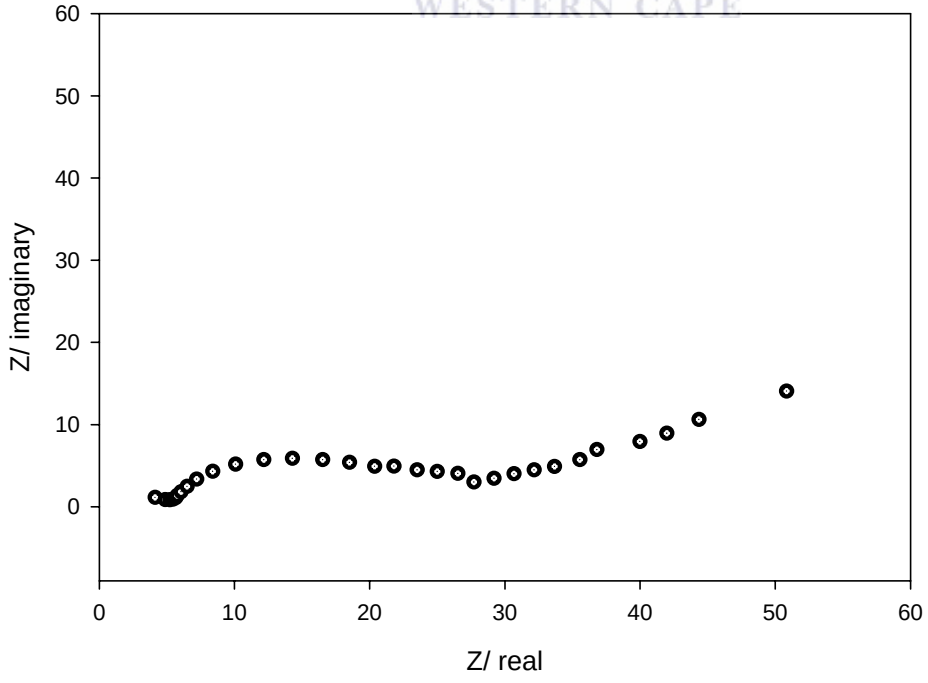

Figure 4.24. Impedance spectroscopy of PANI-PSSA-FA

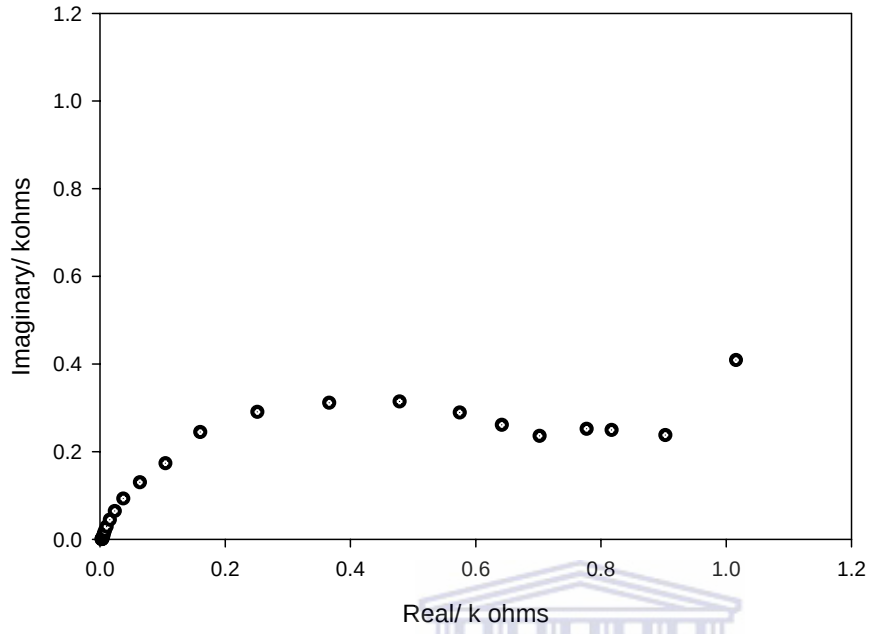

Figure 4.25. Impedance spectroscopy of PANI-PSSA-FA aged

UNIVERSITY of the
WESTERN CAPE

Equivalent Circuit

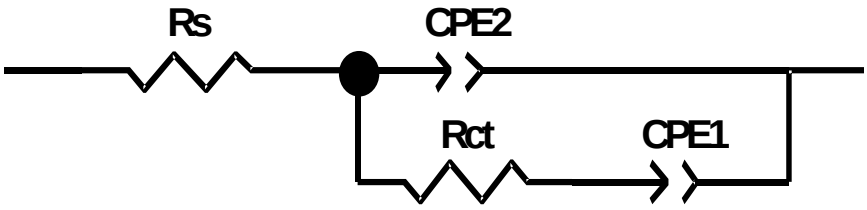

(a)

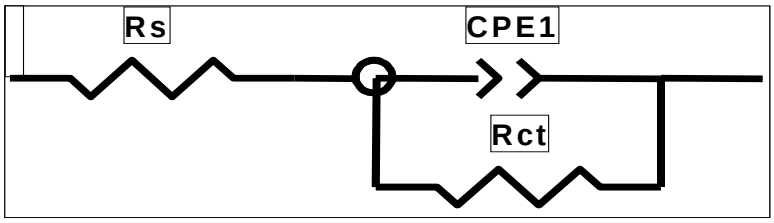

(b)

Figure 4.26 the equivalent circuit of the impedance data.

The impedance spectroscopy and their corresponding circuits are shown in pictures above. PANI, PANI-PSSA-FA aged, and PANI-PSSA-FA correspond to the circuit on Figure 4.25 (a). PANI-PSSA, PANI-FA and PANI-FA aged correspond to the circuit on Figure 4.25 (b). The presence of CPE indicates that the roughness of the electrode [34-36]. This was expected because we were working with paste so the contact between paste and electrode was not homogeneous. The CPE fitted better than the Warburg impedance. It must be remembered that the CPE behaves like the Warburg impedance if it about 0.5, which agrees with the cyclic voltammetry results.

UNIVERSITY of the
WESTERN CAPE

The impedance results show that all composites are conductive and the presence of FA lowers the conductivity. This can be clearly observed in PANI-FA composites where the solution resistance is lower in the absence of FA and higher in the presence of FA. This is in conformation with cyclic voltammetry findings. The presences of decompressed semicircles are an indication of conductive system [30].

4.1. Scanning Electron Microscopy (SEM)

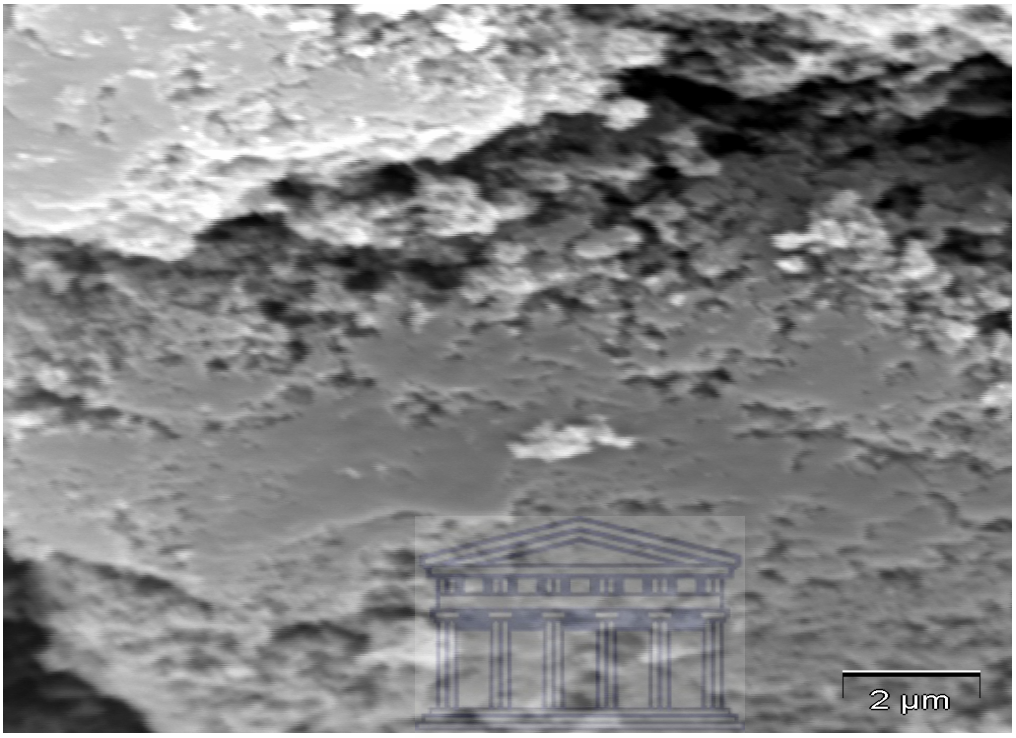

(a)

UNIVERSITY of the
WESTERN CAPE

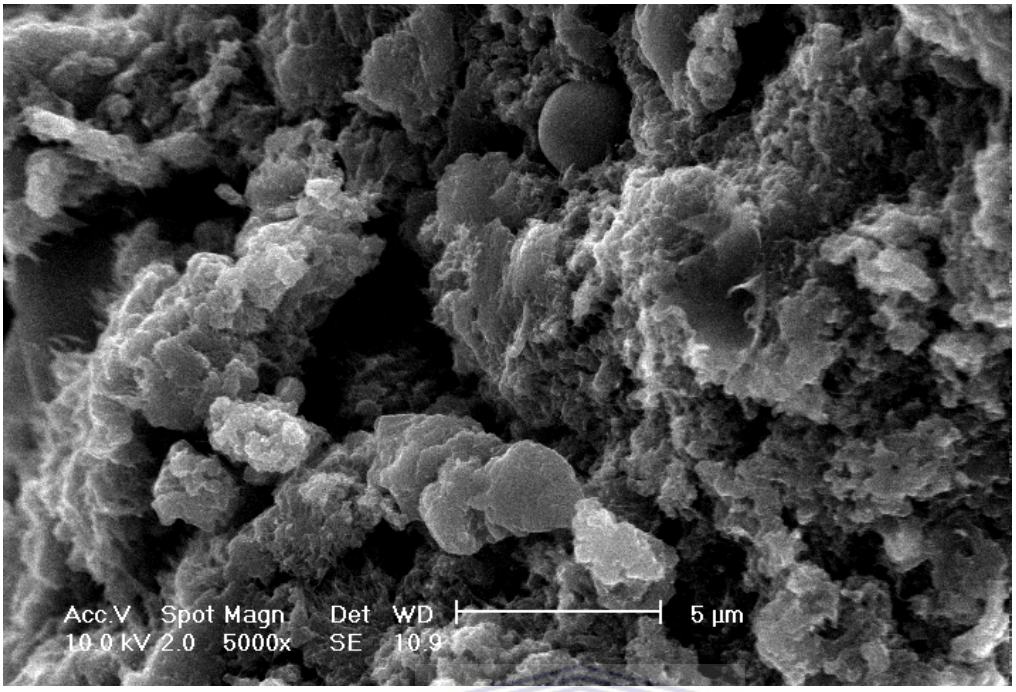

(b)

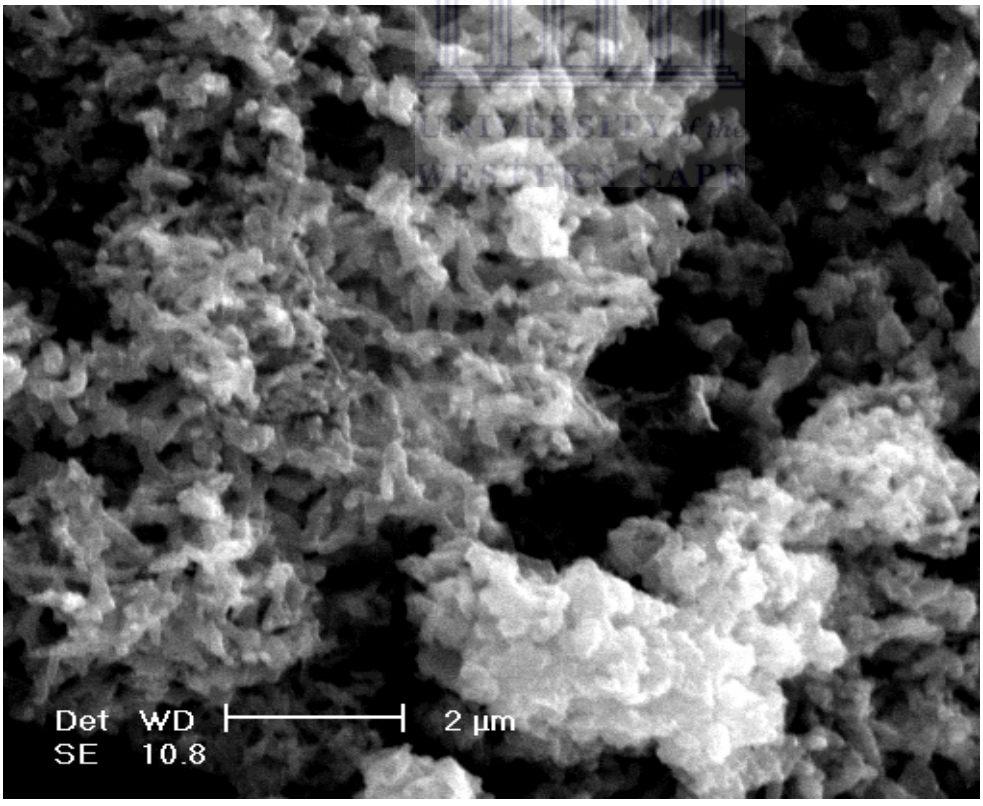

(c)

UNIVERSITY of the
WESTERN CAPE

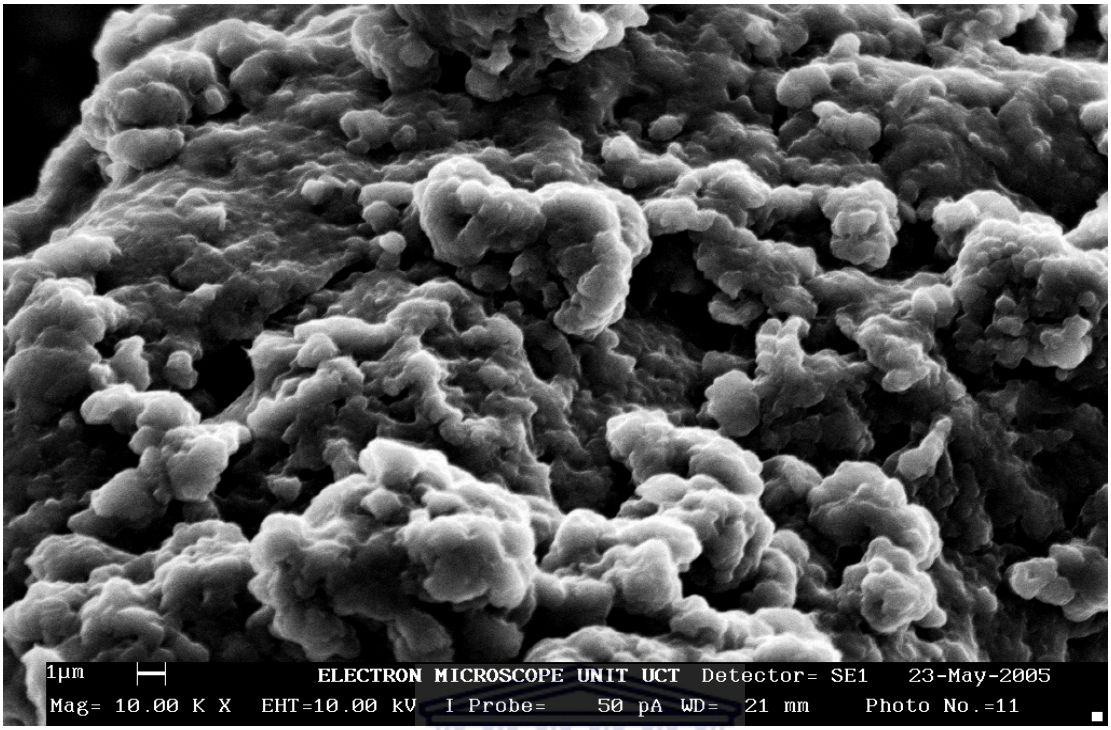
1µm
ELECTRON MICROSCOPE UNIT UCT Detector= SE1 23-May-2005
Mag= 10.00 K X EHT=10.00 kV I Probe= 50 pA WD= 21 mm Photo No.=11

(d)

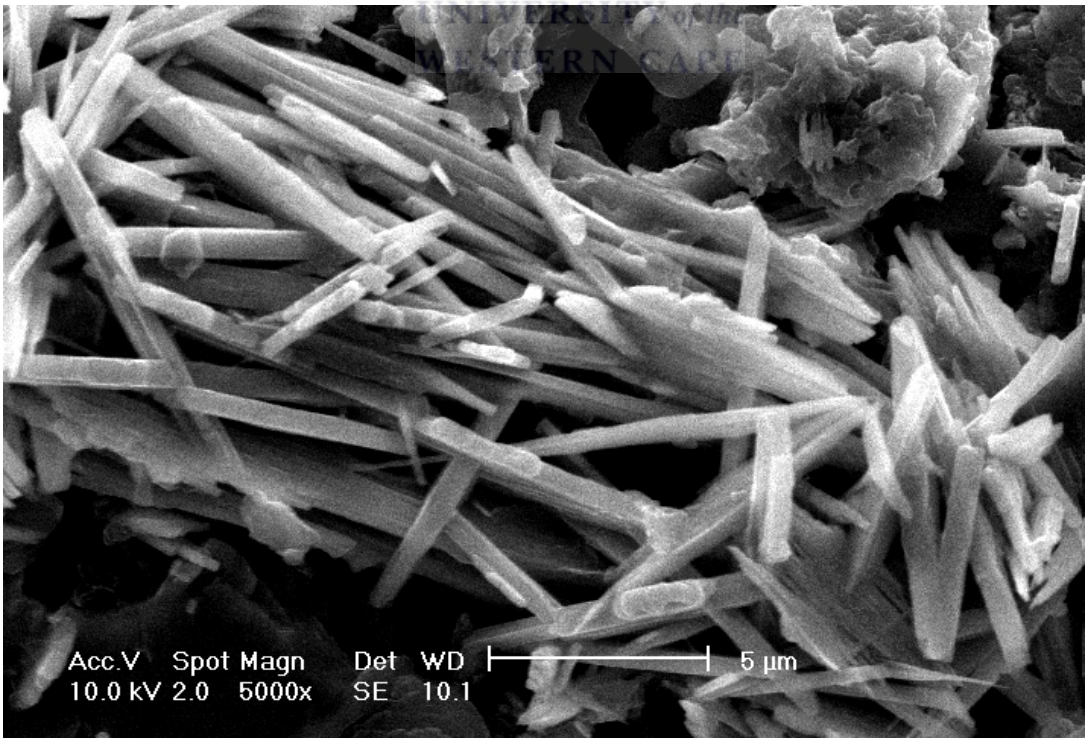
Acc.V Spot Magn Det WD 5 µm
10.0 kV 2.0 5000x SE 10.1

(e)

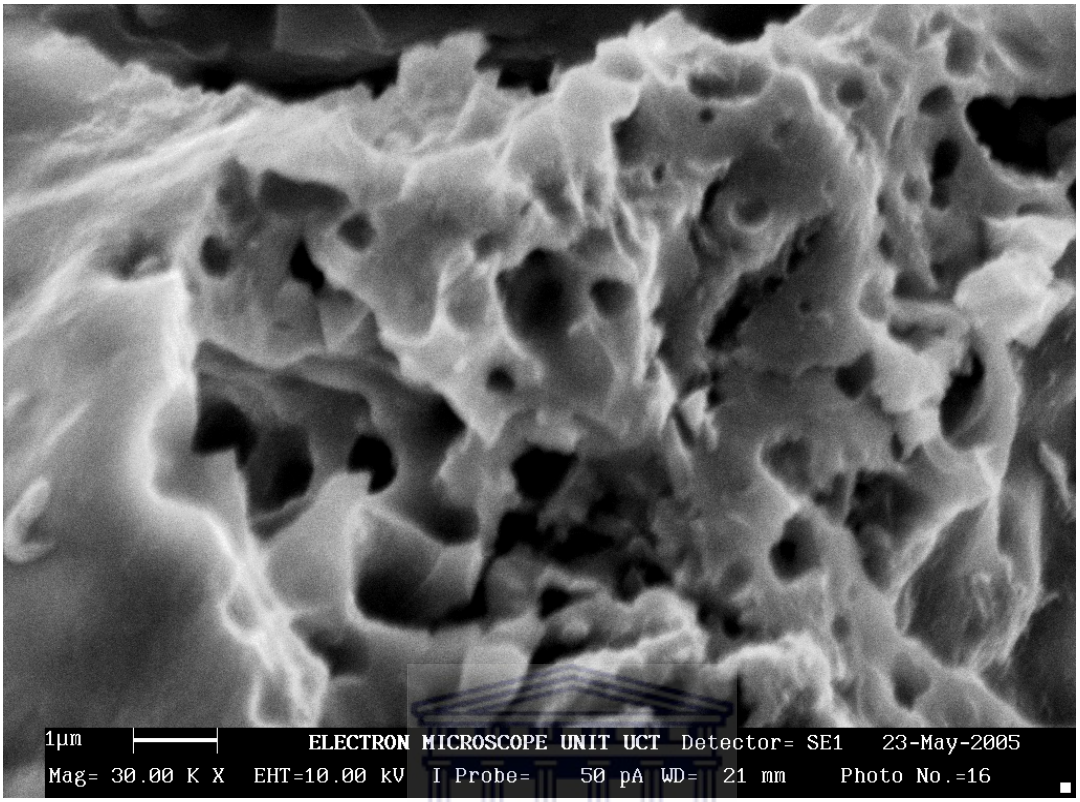

(f)

Figure 4.27. (a) PANI, (b) PANI-FA, (c) PANI-FA aged, (d) PANI-PSSA, (e) PANI-PSSA-FA, and (h) PANI-PSSA-FA aged

The scanning electron microscopy images of the composites are displayed in Figure 4.27. Figures 4.27 (a)-(c) represent PANI, PANI-FA and PANI-FA aged composites respectively. It is seen from Figures 4.27 (b) and (c) that the PANI-FA composite is not highly homogeneous. Whereas the PANI-FA aged composite has a very good homogeneous morphology and some fibber like materials are also visible. These fibbers may be due to the presence of different transitional metals, which indicates better potential of forming nanotubes. Huang [22] reported the formation of nanotubes in the spheres of silica (SiO2). This was due to large curvature of silica structures. The formation of fibbers in PANI-FA aged Figures 4.27 (c) may be due to the polymerisation

in of aniline in the curvature of silica. This happed when the FA and aniline were aged at 100 ^{0}C for 48 hours, which gave aniline time to penetrate into silica spheres.

Figure-5 (d) to (f) represents PANI-PSSA, PANI-PSSA-FA, and PANI-PSSA-FA aged composites respectively. Here it is found that the PANI-PSSA composites have spherical particles of which some of them are micelles like. When FA is added nanorods are produced which is visible form Figure-5 (e). The rods may have been formed by self-assembly mechanism described by Zhang et al. [23]. Because PSSA has Sulphonic groups (-SO_3H) which can act as surfactant, it is easy for it to form micelles. With the presence of metal oxides it may produce rods shaped composites. In case of composites, which were aged, gives a film like surface with holes.

UNIVERSITY of the
WESTERN CAPE

4.6. Thermal Gravimetric Analysis

Below are the TGA results of PANI composites with FA.

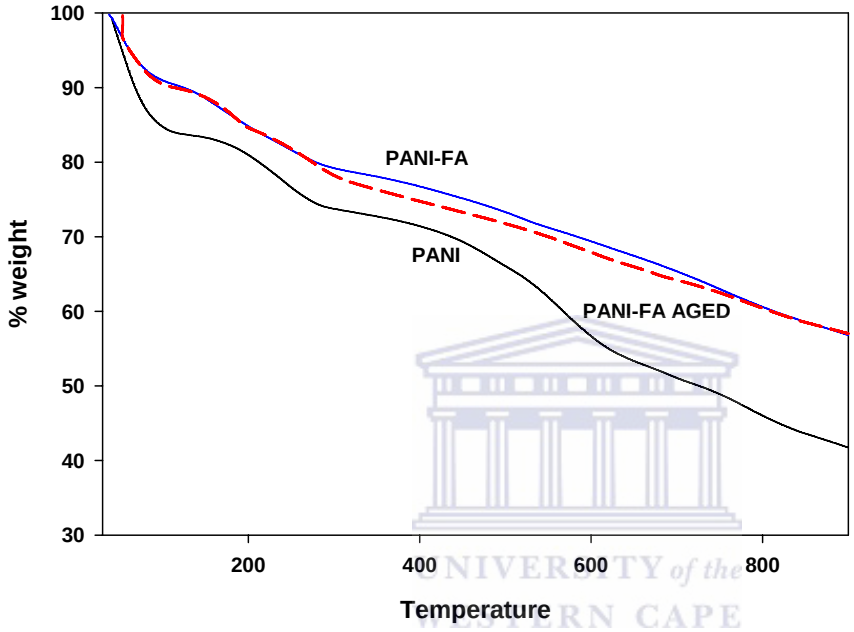

Figure 4.28 TGA of PANI-FA composites

UNIVERSITY of the WESTERN CAPE

Below are the TGA results of PANI-PSSA with FA.

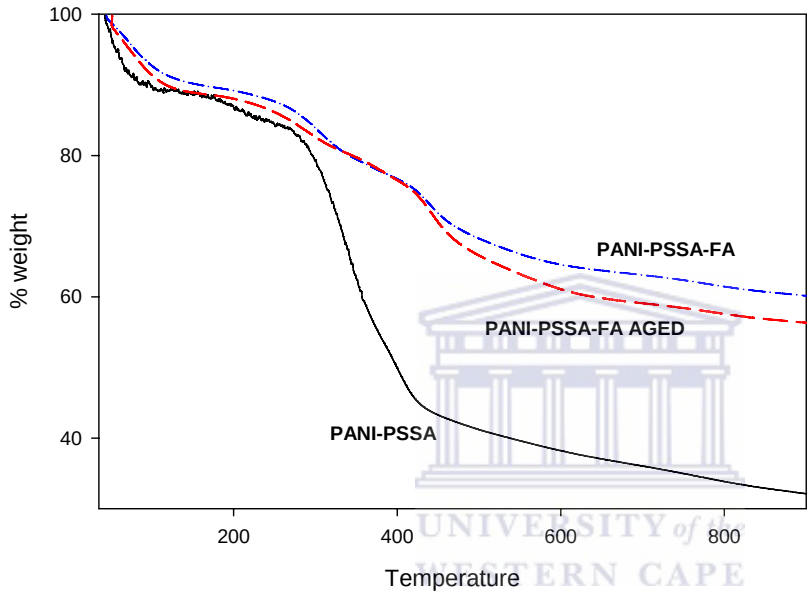

UNIVERSITY of the
WESTERN CAPE

Figure 4.29. TGA results of PANI-PSSA-FA composites

From the TGA thermmograms (Figure-4.28) we found three-step decomposition of PANI. The initial weight loss up to 120 ^{o}C may be due to the removal of moisture present in the polymer. A small amount of weight loss in between 160 ^{o}C to 240 ^{o}C suggest that the polymer still contains some volatile materials most probably HCl. The onset temperature of the degradation of PANI is observed to be around 420 ^{o}C accompanied by massive weight loss towards higher temperature [9,10]. In PANI-FA and PANI-FA-aged

composite three steps degradation is also observed. Initial weight loss up to 100 ^{o}C may be due to the loss of moisture and further weight loss up to 200 ^{o}C may be associated with the removal of volatile material most probably HCl trapped within composites. There is a moderate weight loss from 500 ^{o}C may be associated with the degradation of the polyaniline back bone of the composites, then the composites shows a very slow degradation towards higher temperature may be due to the presence off different metal oxides of FA within the composites and may be due to the formation of different complexes between the metal oxides and polymer back bone at higher temperature.

From Figure 4.29 we found a three-step degradation of PANI-PSSA composite. Initial weight loss up to 100 ^{o}C may be due to the removal of the moisture within the materials and the second stage a very slow weight loss between 180 to ~220 ^{o}C may be associated with the removal of volatile materials most probably HCl and some PSSA. Then a massive weight loss from 350 ^{o}C up to 420 ^{o}C corresponds to the degradation of the polymer backbone. In case of PANI-PSSA-FA composites the first two-step of weight loss is due to the same region as in case of PANI-PSSA composite. But in the third step there is a weight loss from 450 ^{o}C, which may be associated with the degradation of polyaniline. After that the degradation process is slow towards higher temperature and may be due to the formation of different complexes between the metal oxides of FA and the polymer back bone during the heating process. But one thing is clear from the thermmograms, is that the composites have better thermal stability as compared to polyaniline [8,9].

UNIVERSITY of the
WESTERN CAPE

Table 2. Summary of TGA of PANI-FA composites analysis

	Evaporation of water (^{0}C)	**Evaporation of adsorbed water and HCl (^{o}C)**	**Degradation of polymer backbone (^{o}C)**
PANI	120	160	**420**
PANI-FA	120	140	**500**
PANI-FA aged	120	140	**500**

Table 3. Summary of TGA of PANI-PSSA-FA composites

	Evaporation of water (^{o}C)	**HCl and PSSA degradation (^{o}C)**	**Degradation of polymer backbone (^{o}C)**
PANI-PSSA	100	200	**350**
PANI-PSSA-FA	100	340	**420**
PANI-PSSA-FA aged	100	340	**420**

UNIVERSITY of the
WESTERN CAPE

CHAPTER 5

CONCLUSIONS

We have successfully synthesized the PANI –FA composites with different ratios of FA to aniline. Our modified methods were also successfully demonstrated. The two peaks at 1558 and 1469 cm^{-1} from the FT-IR affirm the presence of quinoid and benzoid rings, which are characteristics of polyaniline backbone.

Both FT-IR and UV-Vis data were in close agreement about the formation of doped composites. This was demonstrated by the peak at 450 nm in UV-Vis, which is the indication of doped polyaniline. The position of the quinoid and benzoid rings peaks at 1469 and 1558 cm^{-1} confirms the doped state polyaniline because the undoped polyaniline has these peaks between 1590-1600 cm^{-1} and 1500-1490 respectively.

UNIVERSITY of the
WESTERN CAPE

FT-IR gave the peaks at 1143-1136 cm^{-1}, which are the measure of delocalisation, which means that the materials were conductive. The presence of decompressed semi-cycles from EIS is an indication of the conductive system. Cyclic voltammetry also confirms that the composites were conductive and the hoping of electrons happened along the polymer backbone. This was evident due to the shifting of the anodic peaks to the higher potential as the scan rate increases. Cyclic voltammetry also showed that the composites were electroactive and showed reversible electrochemistry. This was also confirmed by the calculation of standard rate constant.

The results demonstrate that the composites which formed nanorods and fibbers (PANI-PSSA-FA 40 and PANI-FA 40 aged) had very good electrochemistry. These composites showed better reversibility than the other composites, which were synthesised using the same method. PANI-FA 40 aged had k^0 greater than for PANI-FA 40 and also PANI-PSSA-FA had greater k^0 than PANI-PSSA-FA 40 aged. This means that these two composites (PANI-FA aged and PANI-PSSA-FA 40) can exchange electrons rapidly without significant molecular reorganization. The high diffusion co-efficient (D) values also showed that the two mentioned composites could transfer electrons faster than their counterparts.

The TGA results showed that the presence of FA in the composites could improve the thermal stability up to 100 ^{0}C. Without FA PANI backbone start degrading at 420 ^{0}C but when PANI has FA it decomposes at 500 ^{0}C. PANI-PSSA also improves from 350 to 420 ^{0}C with the presence of FA.

UNIVERSITY of the
WESTERN CAPE

This study also showed that conductivity is lowered by presence of FA. This was demonstrated by the shift of PANI peak from 360 nm to 330 nm when there is Fly Ash present in the composite. This was also observed in PANI-PSSA-FA composites where the PANI-PSSA peak shifted from 385 330 nm. This showed that FA can be used to control the conductivity of PANI to make it suitable for various applications.

The modified method of PANI-FA composites showed that by putting reaction under heat can help make FA reacts better and forming homogeneously mixed composites. This method also demonstrated that nanocomposites with fibbers could be synthesized by changing the conditions of the reaction. The presence of a post peak in Cyclic voltammetry of PANI-FA 40 indicated that when FA is not heated it formed inhomogeneous materials with some unreacted FA, this is also observed in SEM where FA particles are visible from the unmodified PANI-FA method. The other modified method of PANI-PSSA-FA composites showed homogenous materials with PANI-PSSA-FA 40 forming nanorods. The presence of PSSA and metal oxides from FA helped in the formation of nanorods by forming micelles which act as template for the formation of nanorods. In the absence of FA no nanorods were formed.

UNIVERSITY of the
WESTERN CAPE

In this study we have shown how a potential toxic waste like FA can be used to produce product that have potential applications. It is clear from this study that nanotubes/rods of PANI can be formed with FA. These composites can be used in photo electrochemical systems due to combination of n-type semiconductor of transitional metals and p-type of PANI, which are thought to cause improvement in photo current values of polyaniline due to the occurrence of excitons dissociation at the interface. These composites can also be used in biosensors because of their good reversible electrochemistry. Their high thermal stability and the ability of polyaniline to switch from a conductor to insulator make them potential candidates for use as anticorrosion materials in the mining industry.

REFERENCES

1. B. Norden and E. Krumeirjer; Noble prize in chemistry, 2000: conducting polymers; **2000**; the royal Swedish Academy of science; [online] www.kva.se

2. A. Pud, N. Orgurtsov, A. Korzhenko, and G. Shapoval; **2003**; Some aspects of preparation and properties of Polyaniline blends and composites with organic polymers; Progress in Polymer Science; (28); pp 1701-1753.

3. J. E. Albuquerque, L. H. C. Mattoso, D. T. Balogh, R. M. Faria, J.G. Masters and A.G. MacDiarmid; **2000**; A Simple way to estimate the oxidation state of polyanilines; Synthetic metals; 113; pp19-22.

4. S.C. Raghavendra, Syed Khasim, M Revanasiddappa, M V N Ambika Prasad and AB Kulkarn; **2003**; Bull.Mater. Sci; (26); pp 733-739.

5. M. S. Cho, Y. Park, J. Yeong, and H. J. Choi; **2004**; Synthesis and electrical conductivity of polymer composites with polyaniline nanocomposites; Material Science and engineering; 24; pp 15-18.

6. Fritz Huguenin, M Janete Giz, Edson A Ticianelli, Roberto M. Torresi; **2001**; Structure and properties of a nanocomposites formed by vanadium pentoxide containing poly (N-propane Sulphuric acid aniline); Journal of power sources; 103; pp 113-119.

7. M. Kanungo, A. Kumar, and A. Q. Contractor; **2003**; Micromolecule Sensors and Sensor Array Based on Polyaniline Synthesized in the presence of Poly (styrene sulfonate); Analytical Chemistry; (75); pp 5673-5679.

UNIVERSITY of the WESTERN CAPE

8. Q H Zeng, D Z Wang, A B Yu and G Q Lu; **2002**; Synthesis of polymer-montmorillonite nanocomposites by in situ intercalative polymerization; Nanotechnology; 13; pp 549-553.

9. L. Zhang, M. Wan; J. Phy. Chem; 107; (2003); pp 6748-6753.

10. D. C. Schnitzler, M. S. Meruvia, I. A. H. Mmelgen, and A. J. G. Zarbin; **2003**; Preparation and Characterization of Novel Hybrid Materials Formed from (Ti,Sn)O2 Nanoparticles and Polyaniline; Chemistry of Materials; (15); pp 4658-4665.

11. C. Wu, Y. Liu, and S. Hsu; **1999**; Assembly of Conducting Polymer/Metal Oxide Multilayer in One Step; Synthetic metals; (102); pp 1268-1269.

12. P.K. Khanna, S. P. Lonkar, V. V. V. S. Subbarao, and K. Jun; **2004**; Polyaniline-CdS nanocomposite from organometallic cadmium precursor; Materials Chemistry and Physics; (87); pp 49-52.

UNIVERSITY of the
WESTERN CAPE

13. R. L. N. Chandrakanthi and M. A. Careem; **2002**; Preparation of CdS and Cu2S nanoparticles/polyaniline composites films; Thin Solid Films; (417); pp 51-56.

14. Nayana chandrakanthi, M. A. Careem; **2000;** Preparation and Characterization of fully oxidized form of polyaniline; Polymer Bulletin; 45; pp 113-120.

15. C. M. A. Brett and A. M. O. Brett; **1993**; Electrochemistry Principles, Methods, and Applications; Oxford Science Publications; Chapter 11.

16. L F Petrik, R White, M Klink, V. Somerset, D. Key, E. Iwuoha, C. Burgers and M V Fey; 2003; Water Research Commission (WRC) of South Africa. Final Report No K5/1242.

17. S. Mavundla; **2003**; Unpublished Honours; University of the Western Cape; Chemistry Department.

18. A. A. Landman and D. de Waal; **2004**; Bulletin of Material Science; 39; pp 665-667.

19. Science in the news; **2000**; Putting it together-The science and technology of composite materials; Australian academy of science; [online] www.science.org.au.

20. Ana K. C. Gallegos; **2003**; Organic/Inorganic hybrid based on conducting polymers as electrodes for energy storage; Unpublished PhD Thesis.

21. Wei Di; **2003**; electro polymerization of N-substituted Aniline derivatives in Organic Media and their Spectroscopic Characterization; Unpublished Masters Thesis; Abo Akademi University.

22. S. Haung; **2003**;Growing Carbon Nanotubes on Patterned sub-micron size SiO_2 Spheres; Carbon; (41); pp 2347-2352.

23. W. Li, P. A. McCarthy, D. Liu, J. Huang, S. Yang, and H. Wang; **2002**; Toward Understanding and Optimizing the Template Guided Synthesis of Chiral Polyaniline Nanocomposites; Macromolecules; 35; pp 9975-998.

24. Z. Zhang, Z. Wei, and M. Wan; **2002**; Nanostructures of Polyaniline Doped with Inorganic Acids; Macromolecules; pp 5937-5942.

25. Y. Wang, Z. Liu, B. Han, Z. Sun, Y. Huang, and G. Yang; **2005**; Facile Synthesis of Polyaniline Nanofibers Using Chloroaurate Acid as an Oxidant; Langmuir; 21; pp 833-836.

UNIVERSITY of the
WESTERN CAPE

26. Z. Zhang, Z. Wei, L. Zhang and M. Wan; **2005**; Polyaniline and their dendrites doped with different Sulfonic Acids; Acta Materials; 53; pp 1373-1379.

27. P. Holister, T. E. Harper, and C. R. Vas; **2003**; Nanotubes; CMP Cientifica.

28. K. Ramanathan, M. A. Bangar, M. Yun, W. Chen, A. Mulchandani, and M. V. Mnyung; **2004**; Individual Addressable Conducting Polymer Nanowires Array; Nano letters; 4; pp 1237-1239.

29. N. G. R. Mathebe, Aoife Morrin, and Emmanuel I. Iwuoha; **2004**; Electrochemistry and scanning electron microscopy of polyanilne/peroxidase-based biosensor; Talanta 64; pp 115.

30. J. Bard and L. R. Faulkner; 2001; Electrochemical methods, Fundamentals and Applications 2nd Edition; John Willey & Sons, INC; Chapter 10.

UNIVERSITY of the
WESTERN CAPE

31. A. J. Bard and L. R. Faulkner; 2001; Electrochemical methods, Fundamentals and Applications 2nd Edition; John Willey & Sons, INC; Chapter 10.

32. W. J. Bae, K. Hyeong, W. H. Jo, and Y. H. Park; **2004**; Exfoliated Nanocomposite from Polyaniline graft copolymers/Clay; Macromolecules; (37); pp 9850-9854.

33. H. Bodugoz, O. Guven; **2005**: Radiation induced Dehydrochlorination as an in-situ Doping Technique for Enhancement of the Conductivity of Polyaniline Blends; Nuclear Instruments and Methods in Physics Research: Articles in Press.

34. D. Hui, R. Alexandrescu, M. Chipara, I. Morjan, Gh. Aldica, M.D. Chipara, and K.T. Lau; **2004**; Impedance Spectroscopy studies on doped polyanilines; Journal of Optoelectronics and advance materials; (6); pp 817-824.

35. P. Zanello; Inorganic electrochemistry: Theory, practice and application; The Royal society of Chemistry; 2003; Ch 1and 2.

36. W. J. Bae, K. Hyeong, W. H. Jo, and Y. H. Park; **2004**; Exfoliated Nanocomposite from Polyaniline graft copolymers/Clay; Macromolecules; (37); pp 9850-9854.

37. M. Kanungo, A. Kumar, and A. Q. contractor; **2003**; Microtubule Sensor and sensor array Based on Polyaniline synthesized in the Presence of Poly (styrene sulphonate); Analytical chemistry; 75; pp 5673-5679.

38. G. M. do Nasimento, V.R.L. Counstantino, and M. L .A. Tempereini; **2002**; Spectroscopic Characterization of a New Type of conducting Polymer-Clay Nanocomposites; Macromolecules; 35; pp 7535-7537.

39. C. Sivakumar, T. Vasudevan, and A. Gopalan; **2001**; Chemical Oxidative Polymerization and in situ Spectroelectrochemical Studies of a Sulfonated Aniline Derivative by UV-Visible Spectroscopy; (40); pp 40-51.

UNIVERSITY of the
WESTERN CAPE

40. Xiaomeng Sui, Ying Chu┌, Shuangxi Xing, Min Yu, Chengzhan Liu; **2004**; Self-organization of spherical PANI/TiO2 nanocomposites in reverse micelles; Colloids and Surfaces; {251}; pp 103-107.

41. Y. Wang, X. Jing; **2005**; Effect of solution concentration on the UV-vis spectroscopy measured oxidation state of polyaniline base; Polymer testing; 24; pp153-156.

42. Y. Xia, J. M. Wiesinger, and A.G. MacDiarmid; **1995**; Camphorsulphonic acid fully doped polyaniline emaraldine salt: Conformation in different solvents by an UV-Vis NIR spectroscopy; Chemical Materials; 7; pp 443-445.

43. S. Pruneanu, E. Veress, I. Mariana, and L. Oniciu; **1999**; Characterization of polyaniline by Cyclic Voltammetry and UV-Vis absorption spectroscopy; Journal of Material Science; (34); pp 2733-27349.

UNIVERSITY of the
WESTERN CAPE

44. L. Huang, T. Wen, and A. Gopalan; **2002**; In situ UV-Vis spectroelectrochemical studies an electrochromic behaviour of poly (2,5-dimethoxy aniline); Synthetic Materials; (130); pp155-163.

45. B. A. Deore, S. Hachey, and M. S. Freud; **2004**; Electroactivity of electrochemically synthesized Poly (aniline Boronic Acid) as a Function of pH: Role of Self Doping; Chemical materials; (16); pp 1427-1432.

46. D. Kim, J. Choi, Y. Han. D. Daewon and J. Kim; **2002**; Size Control of Polyaniline nanoparticles by Polymer surfactant; micromolecules; (35); pp 5314-5316.

47. . Mathew, D. Yang, B. R. Mattes, and M. P. Espe; **2002**; Macromolecules; (35); pp 7575-7581.

48. H. Fischer; **2003**; Polymer nanocomposites: From fundamental research to specific applications; Material Science and engineering; (23); pp 763-772.

49. P. C. Rodrigues and L. Akcelrud; **2003**; Networks and blends of polyaniline and polyurethane: corrections between composition and thermal, dynamic mechanical and electrical properties; Polymer; (44); pp 6891-6899.

50. Z.T. de Oliveira Jr, M.C. dos Santos; **2000**; Relative Stability of Polarons and bipolarons in Emaraldine oligomers: a quantum chemical study; Solid state Communications; (114); pp 49-53.

51. E. Iwuoha, A. R. Williams-Dottin, and L. A. Hall; **2002**; Electrochemical Behavior of polymeric complexes of Monosubstituted Squarate Ligands; Inorganic Acta Chimica; (331); pp 1-7.

UNIVERSITY of the
WESTERN CAPE

Microchim Acta (2006)
DOI 10.1007/s00604-006-0584-z

Microchimica Acta
Printed in Austria

Original Paper

Electrochemical and Spectroscopic Properties of Fly Ash–Polyaniline Matrix Nanorod Composites

Emmanuel I. Iwuoha[1,*], **Sipho E. Mavundla**[1], **Vernon S. Somerset**[1], **Leslie F. Petrik**[2], **Michael J. Klink**[1], **Mantoa Sekota**[1], and **Priscilla Bakers**[1]

[1] Sensor Research Laboratory, Department of Chemistry, University of the Western Cape, Private Bag X17, Bellville 7535, South Africa
[2] South African Institute for Advanced Material Chemistry, University of the Western Cape, Private Bag X17, Bellville 7535, South Africa

Received July 18, 2005; accepted March 18, 2006; published online June 23, 2006
© Springer-Verlag 2006

Abstract. Polyaniline (PANI) nanocomposites were prepared with fly ash (FA) either by aging the starting materials (aniline and FA) before oxidative polymerisation or by including poly(styrene sulphonic acid) (PSSA) eliminating the aging step. The aging procedure formed polymer nanotubes that have cross-sectional diameters of 50–110 nm. The procedure involving PSSA produced nanorods and nanofibres composites that have diameters of 100–500 nm and length of up to 10 μm attributed to the presence of metal oxides and silica in FA. The electrochemical analysis of the PANI–PSSA–FA nanorod composites shows three redox couples with formal potentials, $E^{0\prime}_{(200\,mV\,s^{-1})}$, values of 105 mV, 455 mV and 670 mV, and conductance, C, value of 1.21×10^{-2} S. The UV-Vis spectroscopy of the polymeric nanorod shows absorption maxima at 340 and 370 nm (due to π–π^* transition of the benzoid rings), and 600–650 nm (due to charge transfer excitons of the quinoid structure), which are characteristic of emeraldine base.

Key words: Cyclic voltammetry; fly ash; polyaniline nanorods; polyaniline nanotubes; poly(styrene sulphonic acid); polyaniline-fly ash composites; scanning electron microscopy.

* Author for correspondence. E-mail: eiwuoha@uwc.ac.za

Owing to its high conductivity, environmental stability and low cost of production, polyaniline (PANI) has been the subject of much investigation compared to other conducting polymers [1–6]. Polyaniline can be synthesized chemically or electrochemically in an acidic medium. For chemical synthesis, an appropriate oxidant is required. There are three forms of PANI, namely fully oxidized pernigraniline, half-oxidized emeraldine base (EB) and fully reduced leucoemeraldine base (LB). Emeraldine is said to be the most stable form of PANI and also the most conductive form when doped (emeraldine salt) [7]. Polyaniline is a versatile substance which has potential applications in corrosion prevention, sensors, electronics and electrochromic devices, and batteries [8–12]. However, the processability of PANI continues to be a challenge because of its very low solubility in common solvents and the fact that it decomposes before melting. The complexation of polyanilnes with sulphonic acids {docecylbenzene sulphonic acid, camphor sulphonic acid, poly(vinylsulphonic acid) and poly(styrene sulphonic acid)} has been used as a method of improving the processibility of PANI. Also nanoparticles of PANI have been reportedly synthesized by dispersion polymerization of aniline in the presence of polymeric stabilizers. The

stabilizer absorbs onto the PANI nuclei and prevents the PANI particles from aggregation via steric stabilization. Many polymeric stabilizers have been used recently, including poly (styrene sulphonic acid) (PSSA), poly (vinyl alcohol) (PVA), poly (N-vinyl pyrrolidone), poly (vinyl methyl ether) and methyl-cellulose [10]. Poly (styrene sulphonic acid) is the most commonly used stabilizer. Nanoparticles produced with PSSA as stabilizer exhibit homogeneity in size and morphology, as well as an improvement in conductivity [10]. Another method of making PANI processable requires the incorporation of inorganic materials into PANI moiety to produce polymer nanocomposites. In this regard transitional metal oxides of titanium, cadmium, vanadium and tin have been used to prepare processable PANI nanocomposites [7–9, 13]. These PANI-transitional metals nanocomposites find applications in electronic devices, nonlinear optical systems and photoelectrochemical systems [7, 9]. It is believed that the combination of n-type semiconductor of transitional metals and p-type of PANI is responsible for the improvement in the polyaniline photo current values due to the occurrence of excitons dissociation at the interface [9].

Recently Raghavhendra et al. [1] reported the preparation of PANI–FA composites by *in situ* polymerisation of aniline in the presence of fly ash (FA). The Raghavhendra composites showed decrease in conductivity as the amount of FA increased. South Africa produces a large quantity of fly ash from its coal-fired power plant. Silica (SiO_2), alumina (Al_2O_3), iron oxide (Fe_2O_3) and titanium oxide (TiO_2) are major constituents of FA [14–16]. These metal oxides have been used in one way or the other in the preparation of nanocomposites or nanotubes/rods. For example, Al_2O_3 and Fe_2O_3 have been used as catalyst support for the production of nanotubes [7–9], and Huang [17] reported the growing of nanotubes on the large curvature of silica sphere surface by the pyrolysis of silica and iron(II) phthalocynanine. In this paper we report a new method for the preparation PANI–PSSA–FA composites which forms nanorod and nanofiber morphologies.

Experimental

Materials

Aniline (25% v/v in water), acetone, ammonium persulphate, dimethylformamide (DMF), hydrochloric acid and poly(styrene sulphonic acid) were all products of Sigma-Aldrich Chemicals. Only freshly vacuum-distilled aniline was used for the synthesis of polyanilines. Fresh fly ash samples were obtained from Matla Power Station in South Africa. X-ray diffraction (XRD) studies showed that the main constituents of the Malta FA used in this study are silica ($SiO_2 \sim 50\%$), alumina ($Al_2O_3 \sim 30\%$), calcium oxide ($CaO \sim 5\%$), iron oxide ($Fe_2O_3 \sim 4\%$), magnesium oxide ($MgO \sim 2\%$) and titanium oxide ($TiO_2 \sim 2\%$) [14].

Synthesis of Polyaniline-Fly Ash Composites

The procedure for the synthesis of PANI–FA composites was a modification of the Raghavhendra method [1]. A 0.1 M aniline was prepared in 2 M HCl solution. 100 mL of the aniline solution was stirred and 40% (w/w) FA was added while stirring vigorously. The mixture was kept in an ice bath with continuous stirring. Then 0.1 mol of ammonium persulphate (APS) was added slowly to the aniline solution until the reaction mixture turned green. The reaction mixture was then stirred for 8 h. The product was collected by filtration and washed with water and acetone until the filtrate was colourless. The product was dried at room temperature. For the synthesis of Aged PANI–FA composite, the 0.1 M aniline solution containing 40% FA was kept in the furnace for 48 h at 100 °C. Then the mixture was cooled in an ice bath kept at 0–5 °C while stirring vigorously. After 30 min 8 mL of 0.1 M aqueous solution of APS was added slowly with constant stirring of the reaction mixture. The reaction mixture was stirred for another 5 h and placed in the ice bath for another 5 h. Then the vessel was removed from the ice bath and left at room temperature for 12 h. The product was collected by filtration and washed and dried as described before. The synthesis of PANI–PSSA was in accordance with the method reported by Cho et al. [2]. 10.93 mL of PSSA was dissolved in 555 mL of water to which 9.3 mL of 2 M HCl and 10.68 mL of aniline were added and placed in an ice bath with continuous stirring. 13.84 g of APS was dissolved in 80 mL of water and was added slowly to the reaction mixture in the ice bath and stirred for 12 h. The product (PANI–PSSA) was collected, washed and dried as previously described. For the preparation of PANI–PSSA–FA the aniline solution also contained 40% FA (w/w) before the APS was added.

Characterisation of Composites

Electrochemical measurements were performed with a BAS 50 W potentiostat {Bioanalytical Systems (BAS), Lafayette, IN, USA}. A 20 mL conventional three-electrode cell system (BAS) which was used consisted of BAS Pt disk (1.77×10^{-2} cm^2) working and Ag/AgCl reference (3 M NaCl salt-bridge type) electrodes, and a platinum wire auxiliary electrode. Prior to use, the Pt electrode was cleaned by successive polishing on aqueous slurries of 1 μm, 0.3 μm and 0.05 μm alumina powder (Buehler, Dorset, UK) followed by thorough rinsing with deionised water and acetone. The deionised water was prepared by passing distilled water through Milli-Q™ water purification system (Millipore). The electrode was then placed in a cell solution containing 0.2 M sulphuric acid and the electrode potential cycled at 50 mV s^{-1} from an initial (E_i) to a switch (E_λ) potential of −1200 to +1500 mV, respectively. Cyclic voltammetry (CV) experiments were performed in a cell system consisting of the working, reference and counter electrodes placed in a paste of PANI composite prepared with 1 M HCl. Typically the electrochemical paste cell system consisted of homogeneous slurries made with 0.05 g polymer composite and 5 mL 1 M HCl. The paste cell was de-aerated for fifteen minutes with argon, and a headspace argon atmosphere was maintained at very low flow rate during analysis. Voltammograms were recorded at 20 °C, scanning anodically ($E_i = -200$ mV and $E_\lambda = +1200$ mV) at potential scan rates of 100–1000 mV s^{-1}.

All the UV-Vis absorbance experiments were performed at room temperature with UV/VIS 920 Spectrometer (GBC Scientific Instruments, Australia) using quartz cuvettes. The UV-Vis sample solution was prepared by dissolving 0.005 g of a PANI composite in 10 mL dimethylformamide. The experimental wavelength was 300 to 800 nm. Scanning Electron Microscopy (SEM) analysis was performed with a Hitachi X-650 Scanning Electron Microanalyser which has an operating voltage window of 5–40 kV. Micrographs were obtained for samples of the composites mounted on aluminium stubs using conductive glue and coated with a thin layer of gold.

Results and Discussion

Morphology of Composites

The scanning electron micrographs of PANI–FA and PANI–PSSA–FA are shown in Fig. 1. The PANI–FA was prepared by aging aniline with 40% FA before polymerisation. The micrographs show that PANI–FA formed nanotube clusters that have average cross-sectional diameters of 50–110 nm. Other preparations where the aniline was not aged with FA did not form nanostructures. The indication is that metal oxides (7–9) contained in the FA activated the self organisation of the polyaniline in tubular morphology. In Fig. 1(b) the SEM micrographs of PANI–PSSA–FA is presented. This was prepared with 40% w/w FA. The inclusion of PSSA caused the aggregation of the polymer-precursors into nanorods that have an average length of 10 μm and cross-sectional diameters of between 100–500 nm. The PANI–PSSA–FA nanorods were prepared without aging the aniline and FA before the addition of the ammonium persulphate. Further studies showed that aging aniline-FA–PSSA mixture before polymerisation did not alter the morphology of PANI–PSSA–FA. This shows that PSSA stabilised the morphology of the composite. However, studies with PSSA and aniline did not produce nanostructured morphology. The conclusion here is that the oxides in fly ash play an important role in determining the nature of the product formed. The UV-Vis and electrochemical behaviour of the PANI–PSSA–FA nanorods will be studied.

a

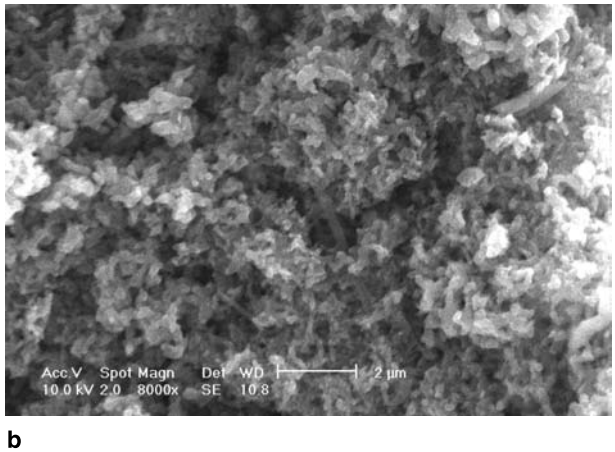

b

Fig. 1. Scanning electron micrographs of (a) PANI–FA (40%) aged. (b) PANI–PSSA–FA (40%)

UV-Vis Spectroscopic Responses

Figure 2 shows the UV-Vis spectra of the polyanilines-fly ash composites. In order to understand the UV-Vis of PANI–PSSA–FA nanorods, the UV-Vis of PANI and other PANI composites were investigated. Figure 2(a) is the spectrum of aged PANI–FA nanotubes and Fig. 2(b) represents the UV-Vis spectrum of PANI–PSSA–FA nanorods. The spectra of these two FA composites show two distinct peaks at around 320 nm and 630 nm. These peaks are characteristic

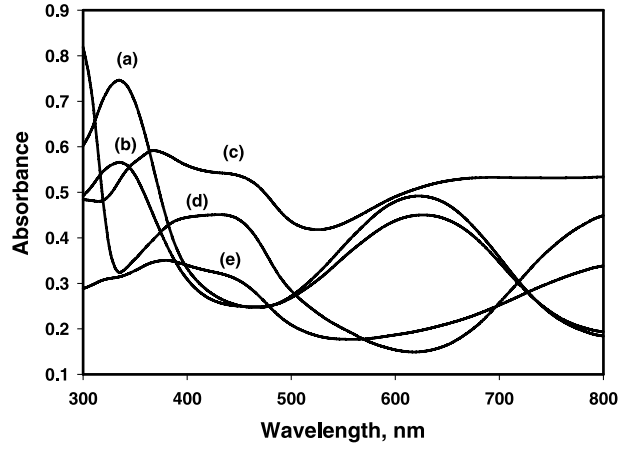

Fig. 2. UV-Vis spectra of polyaniline-fly ash composites with, (*a*) PANI–FA (40%) aged, (*b*) PANI–PSSA–FA (40%), (*c*) PANI, (*d*) PANI–PSSA, (*e*) PANI–FA (40%). Samples were prepared in dimethylformamide

of the PANI emeraldine base [2, 3, 7] and indicate that nanostructured PANI composites are stabilised in the emeraldine base redox state. The peak at 320 nm is attributed to π–π^* transition of benzoid rings and the peak at 630 nm is attributed to the charge transfer excitons of the quinoid structure. Comparatively, PANI–PSSA and PANI–FA prepared without aging show clear similarity in their UV-Vis spectra particularly with the complete absence of the absorption maxima at 320 and 630 nm which is associated with the stabilization of the composite in the emeraldine form. Rather the two composites show absorption peaks at 450 nm and at around 800 nm. The 450 nm peak is due to polarons, and the peak at 680–800 nm is due to the doping level [2]. The peak at 450 nm gives an indication that the PANI is in the salt form (doped). This peak is also observed in pernigraniline salts. Polyaniline that does not contain either PSSA or FA shows four absorption peaks. There are peaks at 340 nm and 370 nm associated with π–π^* transition of benzoid rings and another peak at 600–650 nm (charge transfer excitons of the quinoid structure) which are characteristic of emeraldine base [18]. The peak at 450 nm shows the formation or presence of pernigraniline salt. Comparison of the PANI and PANI–PSSA–FA spectra shows that FA stabilises the polyanilines in its emeraldine form. The electrochemical behaviour of the nanorod composite is presented in the next section.

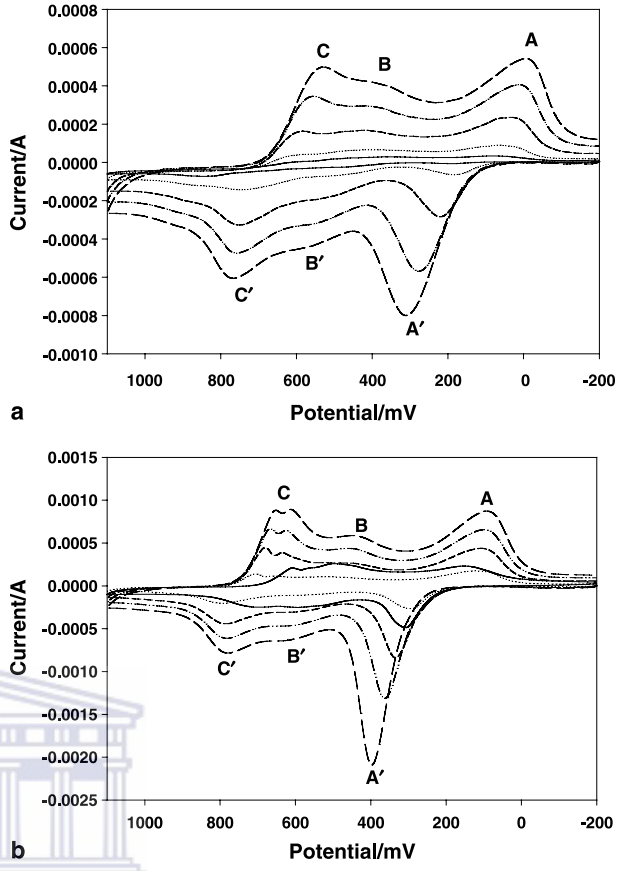

Fig. 3. Multi-scan rate cyclic voltammograms of (a) PANI–PSSA–FA (40%) and (b) PANI–PSSA paste in 1 M HCl performed at of 100, 200, 500, 750 and 100 mV s^{-1} (from inside outwards). (A/A') leucoemeraldine/leucoemeraldine radical cation; (B/B') emeraldine radical cation/emeraldine; (C/C') pernigraniline radical cation/pernigraniline

Electrochemical Properties of PANI–PSSA–FA Nanorods

Cyclic voltammogram of PANI–PSSA–FA is plotted in Fig. 3. The redox peaks in the figure have been assigned using Pekmez formalism [19, 20]: the first redox peak is leucoemeraldine/leucoemeraldine radical cation (A/A′), the second one is the emeraldine radical cation/emeraldine (B/B′) and the third redox peak is the pernigraniline radical cation/pernigraniline (C/C′). From the experimental design the voltammograms represent the electrochemical behaviour of the PANI composite at high potential scan rate. Only electrode processes (electron transfer reaction at the electrode and any accompanying physical or chemical process) that have rate constants comparable to the fast potential scan rates (200–1000 mV s^{-1}) will be discernible in the voltammograms. The 200 mV s^{-1} cyclic voltammogram (CV) of PANI–PSSA–FA have formal potentials, $E^{0\prime}_{(200\,mV\,s^{-1})}$, values of 105 mV (A/A′), 455 mV (B/B′) and 670 mV (C/C′). The corresponding cathodic to anodic peak current ratio, $I_{pc}/I_{pa(200\,mV\,s^{-1})}$, is 'unity' for all the three redox couples. However at higher scan rates (500–1000 mV s^{-1}) the $E^{0\prime}$ value of the A/A′ redox couple vary with scan rate while those B/B′ and C/C′ are independent of scan rate within limits of experimental error of ±10 mV. For example the $E^{0\prime}_{(1000\,mV\,s^{-1})}$ values are 157 mV (A/A′), 465 mV (B/B′) and 660 mV (C/C′). The $I_{pc}/I_{pa(1000\,mV\,s^{-1})}$ values are 0.7 (A/A′), 1.0 (B/B′) and 0.8 (C/C′). These results indicate that the redox species exhibit quasi reversible electrochemistry at scan rates lower than 200 mV s^{-1}. But at higher scan rates the $I_{pc}/I_{pa(1000\,mV\,s^{-1})}$ values of 0.7 for the A/A′ redox couple means that the anodic process represented by A′ consist of electron transfer reaction at the electrode coupled to a diffusion process that is detectable only at fast scan rates, with the result that the anodic currents are higher than the cathodic

currents and $E^{0\prime}$ values shifts anodically with scan rate. The diffusion processes being detected at high scan rates could be intra-paste charge transfer within the electroactive polymer paste or intra-molecular charge transportation along the polymer backbone. The later event is more likely since $\Delta E^{0\prime}\{= E^{0\prime}{}_{(1000\,mV\,s^{-1})} - E^{0\prime}{}_{(200\,mV\,s^{-1})}\}$ value is only 50 mV which is less than 65 mV normally associated with surface-bound electroactive polymers undergoing charge propagation along polymer chain.

Figure 3(b) shows that the electrochemistry of PANI–PSSA is similar to those of PANI–PSSA–FA nanorods. The three redox couples of the $200\,mV\,s^{-1}$ voltammogram display fairly reversible electrochemistry as shown by the $I_{pc}/I_{pa(200\,mV\,s^{-1})}$ value which is approximately unity for each of the redox couples. But at $1000\,mV\,s^{-1}$ when the contribution of other fast processes become evident in the voltammograms, the $I_{pc}/I_{pa(1000\,mV\,s^{-1})}$ value drops to 0.4 for A/A' and increased to 1.2 for C/C'. This shows that charge propagation is more effective when the polymer is in the form of leucoemeraldine radical cation or pernigraniline radical cation, and for the emeraldine or its radical cation, charge transportation does not make significant contribution to the overall current. Changing from PANI–PSSA to PANI–PSSA–FA decreases both $E^{0\prime}{}_{(200\,mV\,s^{-1})}$ and $E^{0\prime}{}_{(1000\,mV\,s^{-1})}$ values. The effect of this is that FA causes a cathodic shift in the $E^{0\prime}$ values of the polymer irrespective of the redox state of the material.

Conductance of the Nanorod Composite

Normal conductivity measurements using a-four pin probe or conductivity cell gives the net conductance of all the components of the material. However, the conductivity or resistance of individual oxidisation state cannot be obtained in this way. This section demonstrates the determination of the conductance profile of all the six redox states of the PANI–PSSA–FA by applying the classical Ohm's relation to multiple potential scan rate cyclic voltammetry. In this approach the conductance, C, is given by $C = \Delta I_v/\Delta E_v$ where $\Delta I_v = I_{p(1000\,mV\,s^{-1})} - I_{p(200\,mV\,s^{-1})}$ and $\Delta E_v = E_{p(1000\,mV\,s^{-1})} - E_{p(200\,mV\,s^{-1})}$. The conductance values of all the redox states of PANI–PSSA–FA in comparison with those of PANI–PSSA are given in Table 1. The average value for all the six redox states is the conductance of the material, which was calculated as 1.21×10^{-2} S for PANI–PSSA–FA and 1.7×10^{-2} S for PANI–PSSA. There is also a general decrease in the conductance of the redox states of the composite on changing from the nanotubular PANI–PSSA to nanorodular PANI–PSSA–FA. These conductance values calculated for the nanocomposites agree with what is reported for similar substances [21, 22]. The data in Table 1 shows that as the nanorod composite is oxidised, $A' \rightarrow B' \rightarrow C'$, the conductance of the polymer composite increases. This trend is related to the formation of pernigraniline redox state which contains polarons that increased the conductivity of the polymeric nanorod. However, the emeraldine redox state (B') exhibited low conductance value in both PANI–PSSA–FA (0.7×10^{-2} S) and PANI–PSSA (0.53×10^{-2} S) compared to the two other redox states. This may be related to the occurrence of π–π^* transition of benzoid rings and the formation of charge transfer excitons of the quinoid structure characteristic of emeraldine which combine to reduce the conductance of the polymer.

Table 1. Electrochemical parameters of PANI–PSSA–FA and PANI–PSSA

Polymer	Redox peak	Conductance/S	$E^{0\prime}{}_{(200\,mV\,s^{-1})}$/mV		$E^{0\prime}{}_{(1000\,mV\,s^{-1})}$/mV	
PANI–PSSA	A'	2.63×10^{-2}	A/A'	205	A/A'	250
	B'	0.7×10^{-2}				
	C'	3.0×10^{-2}	B/B'	525	B/B'	530
	C	1.0×10^{-2}				
	B	0.9×10^{-2}	C/C'	750	C/C'	715
	A	2.0×10^{-2}				
PANI–PSSA–FA	A'	2.1×10^{-2}	A/A'	105	A/A'	160
	B'	0.53×10^{-2}				
	C'	2.4×10^{-2}	B/B'	455	B/B'	495
	C	0.7×10^{-2}				
	B	0.55×10^{-2}	C/C'	670	C/C'	660
	A	1.0×10^{-2}				

A Leucoemeraldine; *A′* leucoemeraldine radical cation; *B* emeraldine radical cation; *B′* emeraldine; *C* pernigraniline radical cation; *C′* pernigraniline.

Conclusion

Polyaniline nanocomposites containing fly ash have been demonstrated to self-organise as nanotubes when aniline is aged with fly ash over a period of 48 h before oxidative polymerisation. However, to eliminate the requirement of aging aniline and FA before polymerisation, PSSA could be included in the reaction mixture. This leads to the self-organisation of the polyaniline composite as nanorod. Both the nanorod and nanotube FA composites of PANI show similarity in their UV-Vis absorption spectra at 320 nm indicating the stabilisation of the nanostructured material in the emeraldine state. The splitting of the conductance values among the redox states of the composite means that the physical properties of the nanorod can be modulated by the application of appropriate electrode potential to make them suitable for specific applications.

References

[1] Raghavendra S C, Khasim S, Revanasiddappa M, Ambika-Prasad M V N, Kulkarn A B (2004) Bulletin Mat Sci 26: 733
[2] Cho M S, Park S Y, Hwang J Y, Choi H J (2004) Mat Sci Engineering 24: 15
[3] Pruneanu S, Veress E, Marian I, Onuciu L (1999) J Mat Sci 34: 2733
[4] Park M-K, Onishi K, Locklin J, Caruso F (2003) Langmuir 19: 8550
[5] Mathebe N G R, Morrin A, Iwuoha E I (2004) Talanta 64: 115
[6] Brahim S, Wilson A M, Narinesingh D, Iwuoha E I, Guiseppi-Elie A (2003) Microchim Acta 143: 123
[7] Chandrakanthi R L N, Careem M A (2002) Thin Solid Films 417: 51
[8] Albuquerque J E, Mattoso L H C, Balogh D T, Faria R M, Masters J G, MacDiarmid A G (2000) Synth Met 113: 19
[9] Schnitzler D C, Meruvia M S, Mmelgen I A H, Zarbin A J G (2003) Chem Mat 15: 4658
[10] Huguenin F, Janete G M, Ticianelli E A, Torresi R M (2001) J Power Sources 103: 113
[11] Samoylov V A, Hao Q, Shirshov M Y, Swart C, Pringsheim E, Mirsky M V, Wolfbeis O S (2005) Sens Actuators 106: 369
[12] Ando M, Swart C, Pringsheim E, Mirsky M V, Wolfbeis O S (2005) Sens Actuators B Chem 108: 528
[13] Khanna P K, Lonkar S P, Subbarao V, Jun K (2004) Mat Chem Phys 87: 49
[14] Somerset V, Petrik L, Iwuoha E (2005) J Environment Sci Health 40: 1627
[15] Somerset V, Petrik L, White R, Klink M, Key D, Iwuoha E (2004) Talanta 64: 109
[16] Somerset V, Petrik L, Etchebers O, White R, Key D, Iwuoha E (2005) Fresenius Environment Bulletin 14: 1074
[17] Haung S (2003) Carbon 41: 2347
[18] Sivakumar C, Vasudevan T, Gopalan A (2001) Spectroscopy 40: 40
[19] Perkmez N, Pekmez K, Yildiz A (1993) J Electroanal Chem 68: 223
[20] Iwuoha E I, de Villaverde D S, Garcia N P, Smyth M R, Pingarron J M (1997) Biosens Bioelectronics 12: 749
[21] Lua X, Xub J, Wong L (2006) Synth Met 156: 117
[22] Long Y, Chen Z, Duval J L, Zhang Z, Wan M (2005) Physica B 370: 121

UNIVERSITY of
WESTERN CAPE